

Control strategies for heat pumps in a residential area under consideration of system operator benefits and grid stability

J. Meiers^{a, ID, *}, M. Ortleb^{a, ID}, D. Jonas^{b, ID}, L. Tadayon^{a, ID}, G. Frey^{a, ID}

^a Saarland University, Chair of Automation and Energy Systems, D-66123 Saarbrücken, Germany

^b Ingenieurbüro Jonas, D-66740, Saarlouis, Germany

ARTICLE INFO

Keywords:

Energy flexibility
Solar heat pump system
Smart-Grid-Ready interface

ABSTRACT

The energy sector faces challenges due to the increasing use of weather-depending renewables in power generation. The resulting fluctuations must be balanced through storage technologies and Demand Side Management (DSM) methods. Heat pumps are generally recognized as shiftable loads for DSM. More and more heat pump manufacturers in Germany are using the Smart-Grid- (SG-) Ready interface, which enables grid operators on the one hand and system operators on the other hand to control heat pumps for the purpose of DSM aiming at either grid power balancing (grid operator friendly) or to increase the self-consumption rate of the residential energy system (system operator friendly). The presented work aims at a compromise between those two goals. To this end, different control strategies for SG-Ready enabled solar and heat pump systems are implemented in a simulation framework and evaluated for a residential area using different key performance indicators. The results show that a control strategy based on a dynamic price signal (*PRBC2*) with rule-based control and well-chosen switching points, taking into account considered building energy systems and environmental conditions used here, represents the best compromise between system operator friendly behavior and grid operator serviceability. The choice of switching points for the heat pump in the course of the price signal is crucial here, and must take into account the consumption and generation profiles of the local residential areas. The fulfillment value of the key indicators considered here for the representative residential area is 63.9%, whereas the value with the reference operating strategy, in which the heat pump is operated exclusively in SG-Ready Mode 2, is only 50.6%.

1. Introduction

Limiting global warming to below 2°C compared to pre-industrial levels and further efforts to limit the temperature increase to 1.5°C are the central components of the 2015 Paris climate agreement. In order to achieve the 2°C goal, according to the IPCC, the budget for cumulative greenhouse gas emissions in the period from 2016 to 2100 worldwide is 760 Gt CO₂ equivalents (eq) and 59 Gt CO₂eq for the 1.5°C goal [1].

However, the volatility in energy generation from renewable energy sources and the uncertainty surrounding the integration of new technologies mean that more flexibility is required on the demand side in order to achieve the best possible coverage of generation and demand. In a conventional, centralized power supply system with a uni-directional flow of electricity from the power plants to the consumers, flexibility is ensured by flexible energy generation plants and large storage facilities.

The increasing installation of renewable energies and the shift towards the electrification of transportation and heating is changing the energy landscape towards a decentralized, bi-directional energy distribution system which is also having an impact on the distribution grids. Peaks in the supply and feed-in of renewable energy into the electricity grids can lead to voltage violations and overloads of lines and transformers and present distribution grid operators with the challenge of ensuring a secure and reliable supply [2]. Low-voltage distribution grids in particular are reaching their capacity limits due to the rapidly growing use of photovoltaics, heat pumps and electric vehicles, which is leading to considerable investment in grid expansion. In this context, flexible use of these systems, including battery storage systems, can help reduce or postpone grid reinforcements. According to a study by the International Energy Agency (IEA), the global expansion of storage capacities in 2030 and in the “Stated Policies” scenario will grow by a factor of 10.8 (from

* Corresponding author.

E-mail address: josef.meiers@aut.uni-saarland.de (J. Meiers).

<https://doi.org/10.1016/j.enbuild.2025.115442>

Received 31 October 2024; Received in revised form 16 January 2025; Accepted 6 February 2025

54 GW to 585 GW) for utility-scale storage and 5 (from 35 GW to 177 GW) for behind-the-meter storage systems compared to 2023 [3].

With the advancement and progress of communication technologies (ICT), a significant amount of flexibility can now be made available on the demand side. In addition, newer decentralized energy sharing concepts are possible to achieve a local balance between energy production and consumption, thereby relieving the distribution and transmission grids. Nevertheless, the distribution grid has a high grid complexity and a relatively low number of integrated communication links. This makes it difficult to apply modern control theories to control the energy flow at distribution grid level especially under real-time requirements. Also due to the limited spread of ICT, legal framework conditions and existing business cases, electricity customers are only offered limited opportunities to participate, which also affects the acceptance of new flexibility market options. In addition, newer decentralized energy distribution concepts are possible, which create a local balance between energy generation and consumption and thus relieve the distribution and transmission grids. In Europe, the concept of renewable energy communities (RECs) was introduced as part of the revision of the Renewable Energy Directive. RECs can be active in both the heat and electricity sectors, provided they are based on renewable energy, but only small and medium-sized enterprises (SMEs), local authorities and natural persons may participate. Renewable energy produced in the RECs' generation facilities can be consumed, stored and sold by the participants. The main purpose of RECs is to create environmental, economic or social benefits for participants [4]. In view of the threat of climate change, many countries have set themselves ambitious targets for the expansion of renewable technologies. In Germany, the German Bundestag passed the Federal Climate Protection Act (FCPA) in 2019 to implement the required reduction in greenhouse gas emissions.

Here, the national climate protection goals are set out in a binding manner and permissible annual emissions are defined for each relevant sector. The building sector plays a decisive role in this, since in 2021 115 million tons of CO₂eq were produced as direct emissions from the combustion of fuels, which corresponds to a share of 15% of the total CO₂eq emissions in 2021 [5]. The report also states that the CO₂eq reduction targets in the building sector have not been met, with 2 million tons of CO₂eq being emitted more than permitted.

Additionally in view of the expansion of electromobility and the conversion of heating systems to heat pumps, there is considerable potential for flexibility in the building sector. In Germany, the new Building Energy Act (GEG 2023) regulates how the country will heat predominantly with renewable energies (RE) in the future. The GEG 2023 aims to increase the share of renewable energies in buildings sustainably and efficiently. New buildings and replacements of old heating systems must use 65% of renewable energy sources, according to the new regulation. The most realistic options for heating under the GEG 2023 are the supply of heat via district heating, where the respective city or municipality ensures that the heat is renewable or alternatively heating with heat pumps (HP), which will probably bring plenty of momentum to the HP market. This in turn leads to more electrical consumers and possible problems in the electrical grid.

Several actors could benefit from this flexibility on the demand side. For example, grid operators and providers of ancillary services could use the potential of households to provide various balancing services and slower reserve products. Electricity marketers can also benefit by using the flexibility of households for arbitrage trading. Grid operators also need flexibility to counteract grid congestion, or they can consider demand-side flexibility to minimize the cost of grid expansion.

Therefore, with the amendment to Section 14a of the German Energy Industry Act (EnWG), distribution grid operators (DGO) will be able to intervene in controllable consumption devices (non-public electric vehicle charging stations, HPs, battery storage systems, among others) and controllable grid connections from January 1, 2024 in order to avoid grid congestion if their maximum reference power exceeds 4.2 kW. In return, the DGO must no longer refuse or delay the connection of heat

pumps or new private charging stations for electric vehicles with reference to possible local grid congestion.

Since the application of advanced control technologies in the distribution grids will probably take some time due to the inadequate equipment of all participants with ICT as explained above, simple control methods are necessary to avoid grid congestions.

For HPs the intervention can be realized via the Smart-Grid-Ready (SG-Ready) interface. A simple interface that can be used to request different operation states of the HP externally. It is controlled via a control box, which receives encrypted switching commands from the grid operator via a Smart Meter Gateway.

The interests of DGO and homeowners are very different. While the former prefer an even grid utilization, for homeowners the energy costs of electricity consumption play a major role and not the power peaks of grid consumption. On the other hand, there are also variables that are of interest to both sides, such as the number of heat pump starts, as their number is associated with electricity consumption peaks and has a negative impact on the expected life time. Both parties see the effects on certain control signal principles as a possible consequence of the study. The results could provide grid operators with guidance for a simple control signal that also represents an acceptable compromise for both stakeholders.

To the best of the authors' knowledge (see Section 3), there is currently no study that examines the influence of HP control with the SG-Ready interface on a residential area using different operation strategies and evaluates these from the point of view of grid serviceability or system operator serviceability.

This article attempts to fill this gap.

Therefore, this article presents a case study that demonstrates the flexible use of HP heating systems, with and without a PV battery storage system, for a representative residential area.

The evaluation is carried out on the one hand with regard to grid-friendly use and on the other hand with regard to plant operator-friendly use. This publication extends the previous work on a single-family house [6] and, building on this, for a representative residential area [7] with regard to a more comprehensive application of operation strategies and more extensive evaluation.

The methodology in the article essentially comprises the following steps:

1. Introduction of the SG-Ready interface and consideration of existing system controls using the SG-Ready interface
2. Explanation of the methodology for modeling a representative residential area for the simulation studies
3. Explanation of the operating strategies investigated using the SG-Ready interface
4. Introduction of evaluation indicators with regard to grid serviceability and operator friendliness
5. Discussion of the results

Based on this approach, the paper is divided as follows.

The next section describes the SG-Ready interface in the context of smart grids and smart buildings. In a top-down view, the requirements of a smart grid and a building automation and control system are shown, which then lead to the requirements and application scenarios of the SG-Ready interface. Section 3 contains the review of research work on the use of the SG-Ready interface. Section 4 introduces basic classifications of solar HP systems. Section 5 describes the methodology for modeling the representative residential area on which the evaluation of the applied operation strategies is based. These operation strategies are explained in Section 6, whereby both grid-supporting and system operator-supporting modes are explained. The evaluation indicators are introduced in the following Section 7. The simulation framework and the software tools used are then presented in Section 8. Section 9 presents and discusses the simulation results. A summary of the main findings and an outlook on further work concludes the contribution.

2. Smart - Grid / Building / Heat Pump

2.1. Smart Grid

Up to now, a uniform and generally recognized definition of the term *Smart Grid* does not exist [8]. However, all attempts of definition of the term *Smart Grid* contain certain characteristics and keywords such as flexible, economic, reliable, accessible, bidirectional power flow and communication.

More than 80% of the expansion of renewable generation capacities takes place in the distribution grid at medium or low voltage level. Due to the fluctuating generation over time, this requires control to ensure grid stability. It is therefore necessary to adapt power consumption to the current power generation. In addition to the generating plants, the consumers must also be controllable. The use of intelligent measuring systems (iMSys) is intended to determine how much electricity the end consumer currently needs and how much is generated. In this way, peak loads can be shifted to less critical time, which saves the need for back-up power plants. The German Federal Ministry for Economics and Energy (BMWi) names the following central applications, in descending order, the control of which contributes to enabling greater flexibility in consumption: charging stations for electric vehicles, HPs, electric storage heating units, refrigeration equipment including air conditioners and white goods (e.g. dishwasher, washing machine).

Factors influencing the provision of load flexibility are the specific household characteristics, cost-benefit ratio, comfort and time availability of the consumer.

To enable the expansion of smart grids, in Germany the installation of iMSys is prescribed by law in the EnWG. By the Act on Metering Point Operation and Data Communication in Smart Energy Networks (MsbG), all installed analogue meters are to be replaced by at least modern measuring devices (MMD), better still by iMSys by 2032 at the latest. According to the MsbG, MMD are a device reflecting the actual electricity consumption and the actual usage time and can be securely integrated into a communication network via a smart meter gateway (SMGW).

In addition to the current meter readings, one has also access to saved values that are displayed on a daily, weekly, monthly or yearly basis. According to this, iMSys must be able to reliably collect, process, transmit, log, save and delete the measured values from measuring devices. This is necessary to be able to process measured values for billing purposes, to enable meter readings to be taken by the consumer and to ensure reliable administration and remote control of the systems by the grid operator. In addition, the respective actual feed-in from generating plants and network condition data are determined in this way.

Germany has so far been one of the laggards in Europe in the SMGW rollout. In this country, around 158,000 of over 51 million metering points were equipped with smart metering systems by 2021 [9]. In Denmark and Sweden, 100% of households were already equipped with smart metering systems in the same year, and at least 98% in Estonia, Spain, Finland, Italy, Luxembourg and Norway [10].

To accelerate the SMGW rollout, the Act to Restart the Digitization of the Energy Transition (Gesetz zum Neustart der Digitalisierung der Energiewende) was passed in April 2023, which currently provides the legal framework for the smart meter rollout. Together with the current amendment of the legal framework for the intervention of the DGO in controllable consumption devices in the event of grid congestion situations, new tasks and business models are upcoming.

Buildings offer a great opportunity to influence power quality and reliability by acting as an energy supplier and consumer in the low-voltage grid. However, free communication protocols must be used to operate the buildings within the smart grid [11].

2.2. Smart Building

Energy storage systems must bridge weather-related bottlenecks in electricity generation from renewable energy sources, which is why buildings are becoming increasingly important as decentralized energy storage systems and building intelligence for efficient and load-dependent energy management. This is also reflected in the EU Buildings Directive EPBD 2018, which sets energy standards for buildings by 2030 and requires the introduction of the *Smart Readiness Indicator* (SRI) to assess building intelligence [12]. To date, only a few studies have been conducted on the use of SRI to assess intelligence in buildings to demonstrate the actual applicability of this metric exemplarily shown in [13,14].

Basically, the automation of a building describes an autonomously working building [15]. According to DIN EN ISO 16484 [16], a Building Automation and Control System (BACS) is the designation of equipment, software and services for automated control, monitoring and optimization as well as for operation and management for an energy-efficient, economical and safe operation of technical building equipment.

The primary goal of the BACS is to operate the building energy system in an energy-efficient, economical and safe manner. In addition, BACS should increase the comfort and ease the everyday life of the users, thereby supporting people in need of help in particular.

However, a smart building is more than just the BACS technology installed in it. Although this is what makes a building smart, the term smart building also describes the ability of a building to react adequately to grid requirements in terms of a stable power distribution system. Buildings must therefore change from passive consumers to active consumers and producers (prosumers), able to adjust their energy consumption according to current energy levels in the grid. This means that in times when large amounts of renewable energies are available, more energy must be consumed, e.g. by storing energy, and when there is shortage of energy in the grid, energy consumption must be reduced. Buildings must therefore become energy-flexible.

However, according to statements by the German Federal Network Agency (BNetzA) [17], house installations are often decades behind the state of the art. Also most parts of the grid are not yet smart [18]. To change this, simple and cheap solutions like the Smart-Grid-Ready (SG-Ready) interface are required.

2.3. Smart Heat Pump - Smart-Grid-Ready interface

HPs can be used as load-variable consumers by switching them on to use electricity that cannot be fed into the local electricity grid and store it in the form of thermal energy to cover heating demand later. In addition, they can also be switched off in a targeted manner to mitigate consumption peaks. The SG-Ready label introduced by the Federal Heat Pump Association in Germany (BWP) [19] helps to identify HPs that can be addressed via a corresponding interface for grid-supportive load management. This interface can be used, for example, by grid operators to control the device. It can also allow the devices to be controlled by the user with the aim of achieving the highest possible level of self-consumption in combination with a PV system [19]. The SG-Ready label refers to electrically driven heating HPs, with or without domestic hot water heating, from the heat sources air, geothermal or water. For certification, the HP must have a controller that covers four operation states (OS) (see Table 1). Planning documents must also be provided for the models and series on how the system must be dimensioned for load management requirements. Domestic hot water HPs, on the other hand, only need a controller that automatically controls an increase in the hot water target temperature for thermal storage purposes. This corresponds to OS 3 for HPs.

Interface-compatible system components must have logic to control the HP that uses two or more of the defined operation states. The setting of the system components must be evident from the documents for

Table 1
Description of SG-Ready operation states [19].

SG-Ready OS	Description
1 (OFF)	This state is downward compatible with the grid utility lock frequently switched at fixed times and comprises a maximum of 2 hours of “hard” blocking time.
2 (NORMAL)	HP runs in energy-efficient normal state with proportional heat storage filling for the maximum two-hour grid utility lock.
3 (BOOST)	HP runs in boosted operation for space heating and domestic hot water. This is not a definite start-up command, but a switch-on recommendation.
4 (FORCED)	This is a definitive startup command, insofar as it is possible within the framework of the control settings. For this state, different control models must be adjustable on the controller for different tariff and utilization models: Variant 1: HP (compressor) is actively switched on. Variant 2: HP (compressor and additional electric heaters) is actively switched on, optional: higher temperature in the heat storage tank.

the corresponding models and series. The control functions must be adjustable so that the following requirements are met: If a signal to disable the HP (OS 1) is set via the digital input, the signal remains active for at least 10 minutes. After the signal has dropped, it may only be activated again 10 minutes later. The same applies to the signal for the start recommendation or for the start command of the HP (OS 3/4). A complete block of the HP may last a maximum of two hours and may be activated a maximum of three times per day [19].

3. Review on SG-Ready control

The SG-Ready label was introduced by the BWP. Dissemination and research work in this area therefore takes place primarily at German and European level. The following literature can be divided into simulation-based, semi-simulation-based and experimental studies.

Extensive work was first carried out by Fischer [20]. In [21] Fischer et al. presented a control strategy using the SG-Ready interface for pooling 284 HPs respecting the variability of the prices on the day-ahead market for electricity. In a two-level control concept, the target value for the purchased electricity for the entire pool is determined at the upper level by solving an optimization problem every minute, whereby the minimization of the costs of purchased electricity is used as the target function. At the lower level, a closed-loop PID controller calculates the SG-Ready state based on the difference between the measured purchased electricity power and the target value. The results show overshooting and oscillations with strong state changes, for which the authors suggest continuous online adaptation of the PID controller parameters.

In another publication, Fischer et al. [22] deal with the flexibility potential of HPs with SG-Ready interface from the grid operator’s point of view. For this purpose, the authors controlled a pool of 284HPs in simulation studies over various time periods between 1 and 360 minutes with the SG-Ready operation states. As a result, a load shifting potential between -0,18 and 10,68 kWh per HP and test cycle was determined. Furthermore, a strong dependence on the season was found - in summer, the load shifting potential was significantly lower than in winter and the changing season.

Lilliu et al. [23] presented a flexibility market model (FlexOffers) for HPs with SG-Ready interface. Using a state model, the critical times of the switching points for the SG-Ready states were determined according to a rule-based approach. These critical times take into account the heating behavior of the HP system and the permitted room temperature range. One focus was on the maximum number of HPs that the control system can aggregate.

Kemmler at al. [24] have developed a hardware-in-the-loop test bench with a HP and thermal energy storage and used it to test the

Table 2
Fullfillment of investigation features.

Publication	SFH	RRA	OS	EI	PVB
Ortleb et al. [6]	●	○	◐ (5)	● (9)	◐
Meiers et al. [7]	○	●	◐ (2)	◐ (3)	●
this article	●	●	● (14)	● (8)	●

Fullfillment: ○: none ◐: partial ●: full.

SFH: Single Family House; RRA: Representative Residential Area.

OS: Operating Strategy (number of); EI: Evaluation Indicators (number of).

PVB: PV Battery Storage System (partial means either none or with, full means considering both).

SG-Ready interface. To do this, they calculated an optimal schedule for the next 24 hours in order to maximize the proportion of self-generated PV energy consumed. They only used operation states 2 (normal) and 4 (forced) and were able to show that the deviations from the planned and optimum schedule amounted to around 3%.

Göbel et al. [25] also used a hardware-in-the-loop test bench to investigate the SG-Ready interface of a HP using a rule-based control algorithm whose aim is to maximize self-consumption. The fourth SG-Ready operation state (FORCED) was not taken into account. While the heating system exists in reality as a hybrid system consisting of a HP and gas boiler, the thermal and electrical consumption model was mapped using a building simulation. The simulation model also includes a PV system and a battery storage system. The authors identified significant disadvantages of the SG-Ready interface, as precise tracking of the HP according to the surplus energy from the PV system is not possible. Nevertheless, there were significant improvements in the proportion of self-used PV energy.

In their analyses of the operation of HP systems with PV battery storage systems in the field, Barashkar et al. [26] demonstrated the positive significance of these systems with regard to increasing the degree of self-utilization. They monitored HP systems with the SG-Ready interface in single-family homes in Germany during the year 2022. According to their evaluations, the HP was set to the increased operation state using the SG-Ready control system after the household electricity was covered with surplus electricity from the PV system and the battery storage was fully charged. The temperature in the DHW area of the buffer storage was increased by an average of 4.1 K and for the space heating water area by 1.8 K.

According to the authors’ assessment, there is currently no study that examines the influence of HP control with the SG-Ready interface on a residential area using different operation strategies and evaluates these from the point of view of grid serviceability or system operator serviceability. This publication extends the previous work on a reference building type with a classified single family house (SFH) [6] and for a representative residential area [7].

The reference building types are classified as SFH15, SFH45 and SFH100 according to the nominal heating demand of 15, 45 and 100 kWh/m²a and assigned to different building insulation standards corresponding to new construction (SFH15, equivalent to passive house standard in Germany), renovated (SFH45) and unrenovated (SFH100) building.

In addition to the operation strategies considered so far, further ones have been examined and additional evaluation indicators introduced and applied in this work. A delimitation of the previous work is summarized in Table 2.

Ortleb et al. [6] evaluated 5 operation strategies on the basis of 9 evaluation indicators using the example of an SFH 45 with a PV battery storage system. These are all evaluation indicators that are also used in this publication. However, one evaluation indicator, the percentage energy cut-off losses of the generated PV power, was no longer used here, as these were abolished with the amendment of the Renewable Energy Sources Act (EEG) in 2023. For this reason, 8 evaluation criteria are used in this article, but are assumed to be complete with regard to the

current legal situation. An overall assessment shows that the operation strategy of optimizing the degree of self-utilization of PV energy (SCO) delivers the best result. The results show that the operation strategies considered and of a single house could not achieve acceptable compromise solutions for system and grid operators - grid-supportive behavior led directly to very disadvantageous results for the system operator, i.e. the homeowners.

In Meiers et al. [7], the model was extended for a representative residential area and a case study was presented that shows the flexible use of HP heating systems without and with a PV battery system. Two operation strategies were presented and compared on the basis of three evaluation criteria. It was shown that a good compromise between grid serviceability and operator serviceability can be achieved for the residential area under consideration if houses with a PV battery storage system are operated in a self-consumption-optimized manner and houses without a PV battery system are operated with an operation strategy according to a standard load profile. If, with this distribution of operation strategies, the proportion of houses with PV battery systems were to continue to increase from 11% to 20%, with the same distribution across the building types, then the RIB would deteriorate to +12%. With a penetration of PV battery systems of 50%, the RIB would even assume a value of +44%.

The review shows that there is only a limited number of articles dealing with heat pump controls using the SG-Ready interface. In these, only individual control strategies were considered. The authors are not aware of a comparison of several operating strategies, in particular the consideration of DGO and system operator convenience. This article attempts to fill this gap.

4. Solar and heat pump systems

In this section, solar HP systems are briefly characterized in order to establish a context for the following chapter in connection with the HP market. Further reading can be found in [27,28], for example. Solar and HP (SHP) systems represent a promising hybrid energy supply concept for a sustainable power supply, space heating (SH) and domestic hot water (DHW) in buildings. In these systems, electric HPs are combined with solar thermal (ST), solar photovoltaic (PV) or both (ST/PV) including hybrid technologies like photovoltaic-thermal (PVT) collectors. So, the term SHP systems covers all combinations of heat pumps and solar energy technologies. PV systems can be supplemented by a battery storage system. For solar thermal HP systems (STHP), Frank et al. [29] have carried out a classification and presented a standardized visualization and designation scheme which was further developed by Jonas [28,30] with special attention on the interaction of thermal and electrical system component parts.

Heat pump systems are fundamentally differentiated according to their source: air, ground or ground water. In principle, there are three types of connection between the ST collector and HP in SHP systems: serial, parallel and regenerative. In the former, the ST collector serves as the source for HP, while in the parallel connection, HP and ST collector supply the buffer storage. All SHP concepts that serve to regenerate the ground temperature are summarized under the regenerative concept. Regarding the combination in SHP systems, PV systems provide electricity to the system or building (household electricity) while ST systems are used to deliver heat to the system [28]. To sum up, solar technologies are used to increase the seasonal performance factor (SPF) of the overall system. On the other hand, SHPs have higher investment costs than conventional heat pumps due to the additional components and may not always be cost-effective depending on the residential application [31]. In the context of smart grids, PV HP systems with battery storage are of particular interest. In this system, the battery storage system and the HP are two controllable loads in one system and increase the flexibility of the overall system. In these concepts, the PV system supplies the HP with electricity. In contrast to STHP systems, the combination and interaction of the first concept is less complex, as, among other things,

an electrical connection is cheaper to realize than a hydraulic one. In such systems, the household electricity is usually covered first by the PV yield before a further surplus is used to charge the battery storage or the buffer storage via the HP. In this article, we look exclusively at air-source HP with PV battery storage systems.

5. Modeling representative residential area

As the building sector is a major energy consumer in many countries, it is the focus of efforts to reduce energy consumption. Numerous research projects have already been carried out to determine its energy requirements. As the energy consumption characteristics of building complexes and residential areas are complex and interlinked, comprehensive models are needed to assess the techno-economic impact of new energy-efficient technologies on buildings and residential areas. Swan and Ugursal [32] have examined modeling techniques and essentially characterized two categories of energy consumption modeling: the “top-down” and the “bottom-up” method.

The top-down modeling approach works on an aggregated level and generally aims to balance the historical time series of energy consumption with the estimated energy consumption. It treats the residential area as an energy sink and does not differentiate between the energy consumption of individual end users. Top-down models determine the impact on energy consumption due to ongoing long-term changes or changes within the residential area, primarily for the purpose of determining supply requirements.

Bottom-up methods are based on hierarchically dis-aggregated component data, which are then combined according to an estimate of their individual impact on overall energy consumption. These can be modeled using statistical methods (e.g. regression, neural networks), on the basis of building physics or as a combination of the two aforementioned as a hybrid approach [33]. They require extensive databases with empirical data (statistical methods) or detailed physical models to enable the mapping of the individual components.

The physics-based building models can in turn be divided into three techniques: Distribution, Archetypes and Sampling [32]. In the Distribution technique, the distribution of end devices is determined using common energy consumption values in order to calculate the energy consumption of each end user. The Sampling technique uses the energy consumption values of actual sample house data as input data for the model. This allows a wide variety of existing homes to be captured. With the Archetype technique- we roughly classify the building stock according to year of construction, size, house type, etc. The energy consumption estimates of the modeled archetypes are scaled up to be representative of the regional building stock by multiplying the results by the number of houses that match the description of each archetype.

In accordance with this classification, the model of a representative residential area is explained below, which was created using the bottom-up model approach. A hybrid model of a residential building is used here. The model part based on statistical data includes the electrical household consumers, which are calculated according to VDI 4655 [34] using an empirical model approach. The building heating demand and the resulting electrical energy demand of the heat pump and the other electrical components of the heating system are based on physical models.

Furthermore, the technique of archetypes is used here, whereby the heat pump and building stock in Germany is classified into standardized heat pump and building types.

5.1. Heat pump market in Germany

According to the BWP, in 2020, the volume of HP sales has increased tenfold since 2000. The upward trend of recent years continued in 2023 and a total of 350,000 HPs were sold, which corresponds to growth of 48% compared to the year before (236,000). Of the HPs sold in 2023,

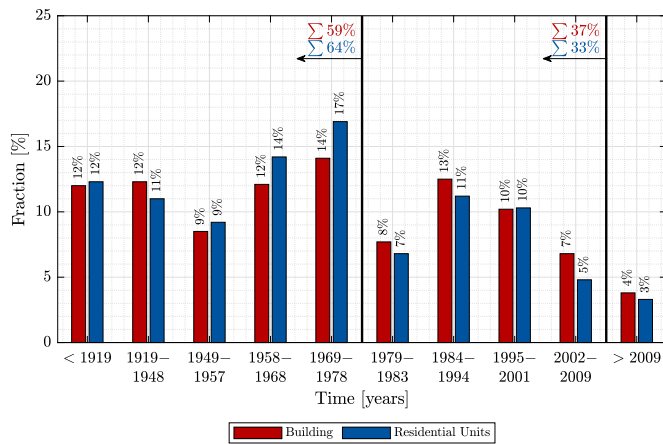


Fig. 1. Age distribution of buildings and residential units in Germany in 2016 [37].

around 87% were air-source HPs. The market situation for brine-to-water HPs is less clear. Sales of these systems have been declining. In 2020 around 22% were brine HPs and only 3% groundwater HPs. For groundwater HPs, a significant increase was recorded, albeit at a low level from 4,000 devices in 2021 to 7,500 devices in 2022. The association expects sales figures for heat pumps to exceed 500,000 appliances in 2024 and to become the new standard heating system in 2030 with an estimated 6,000,000 appliances [35]. In 2021, HP systems were installed in around 54% of all new buildings, making heat pumps once again the most common heating system in the new construction sector. The combination of HP systems and solar systems, such as PV or solar thermal energy, offers great potential for making the energy supply of buildings more self-sufficient. However, the current distribution of such combined systems cannot be determined conclusively. Neither the BWP nor the German Solar Industry Association (BSW) have data on the distribution of solar HP systems. Every federal association collects data on the distribution of its own systems, but there is no interface that records whether a solar system is used to supply a HP.

5.2. Building stock in Germany

The new building ratio (number of new apartments compared to total apartments) in Germany is around 1%, which means that the specifications for energy standards for new buildings have little impact on reducing the overall heating energy consumption of residential buildings. Since in 2020 around 67% of the approximately 42 million residential units in Germany were built before 1979 and thus before the first Thermal Insulation Ordinance came into force, there is a particularly high savings potential in the residential building stock [36].

In a 2018 study, the Institute of Housing and Environment (IWU) conducted a data collection on energy quality and modernization trends in the German residential building stock in 2016. An evaluation of the building age distribution in Germany based on these results is shown in Fig. 1 [37]. Based on this data collection, 59% of residential buildings in Germany were built before 1979 and are thus classified as old buildings. The deviations between the frequency distribution of buildings and apartments are generally not very large. It is noticeable that, especially in the periods 1949-1978, the percentage shares are predominant for dwellings compared to buildings. Here, therefore, the average number of apartments per building is obviously greater than in other building age classes. Based on this data, the German Energy Agency (dena) estimates that 36% of old buildings built up to 1978 have been retrofitted with insulation [38] and thus belong to the group of renovated buildings.

For the building standards introduced in the next chapter, the passive house standard was chosen for new buildings. This building standard

Table 3
Structure of the RRA.

Type of Building	with PV-Battery System	Number of Buildings
SFH100	no	336
SFH100	yes	42
SFH45	no	518
SFH45	yes	64
SFH15	no	36
SFH15	yes	4
Total		1,000

was demanded by the European Parliament for all member states in 2008 and is to be implemented from 2011. According to the data available, all buildings constructed from 2009 onwards (4%) are therefore assigned to the passive house standard. The remaining 37% of buildings (see Fig. 1) are assigned to the building standard of a renovated old building.

5.3. Model of the representative residential area

For simulations within the framework of the IEA SHC Task 44 / HPP Annex 38 (A38T44) [39], different reference building types have been defined and parameterized in order to guarantee uniform simulation heat loads. The focus of A38T44 is on the investigation of SHP systems. The reference heat loads and simulation boundary conditions are defined in two reports - part A0 describes the general simulation boundary conditions including the domestic hot water heat demand, part B0 the reference heating demand scenarios (building) including heat rejection system.

As stated in Section 3 the reference building types are classified as SFH15, SFH45 and SFH100 according to the nominal heating demand of 15, 45 and 100 kWh/m²a.

Taking this classification into consideration and based on the characteristics of HP market and the building stock in Germany described in the two previous subsections, the representative residential area (RRA) explained below is assumed for the further simulation studies.

The RRA consists of 1,000 houses. The building age distribution is derived from the building stock data analyzed in Section 5.2, whereas 590 (59%) of the buildings were built before 1978, of which 212 are renovated, with a renovation rate of 36% as described previously and a rest of 378 buildings are unrenovated. 370 (37%) were constructed between 1979 and 2010 and 40 buildings (4%) from 2010 onwards are declared as new buildings. Accordingly, the following distribution results: 378 buildings are assigned to building type SFH100, 582 to type SFH45 and 40 to SFH15. Since the share of air/water HP system (ASHP) in the market is the highest (cf. Section 5.1), only these used for SH and DHW heating in all of the buildings, which are connected to a certain extent with a PV battery storage system. According to a study by EUPD Research [40], around 1,3 million PV systems were installed on single and two-family houses in Germany by the end of 2020, which corresponds to a share of 11%. This is taken on the occasion of 11% of the buildings of a type with a PV battery system. This results in six different building types in the RRA as shown in Table 3.

Furthermore, the weather conditions in the RRA are assumed to be moderate and the weather data for Strasbourg referred to the IEA Reference Simulation Framework has been applied [39].

6. Control strategies

This section presents the SG-Ready control strategies considered. They can be differentiated into four groups: Self-consumption-optimized control (Subsections A-B), Standard Load Profile-based (SLP) control (Subsections C), Rule-Based Timer Control (RBTC) (Subsections D) and Price and Rule-based control (PRBC) based on day-ahead electricity prices (Subsection E).

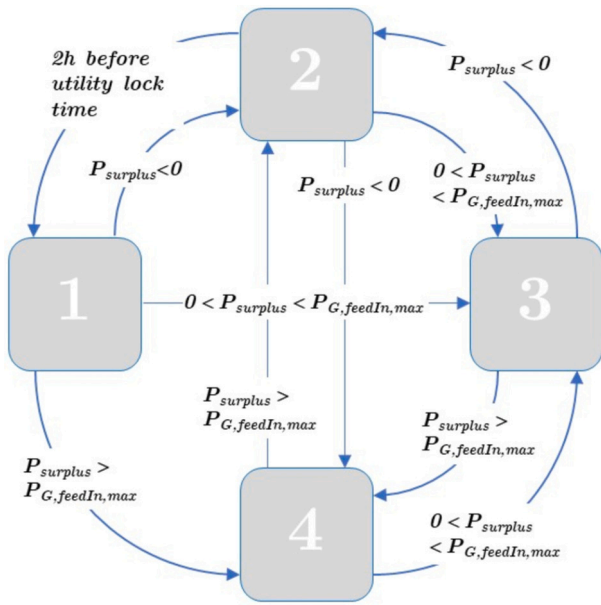


Fig. 2. S10 control algorithm flow chart.

The strategies in Subsections A-B have been described in the literature in outline form before, the others are new contributions.

All heat-map figures show the SG-Ready OS of a SFH45 building with an air-source HP and a PV battery storage system. As presented in section 2.3, the four SG-Ready OSs are as follows:

- OS 1: (OFF):HP is switched off
- OS 2: (NORMAL):HP runs in normal state
- OS 3: (BOOST):HP is recommended to switch on
- OS 4: (FORCED):HP is forced to switch on

6.1. Predictive self-consumption optimized control (S10)

The first operation strategy used is based on the control logic of the E3/DC S10 Energy Management System (EMS) [41] incorporating a PV battery storage system. SG-Ready HP can be connected and controlled by the EMS. As soon as curtailment takes place because the PV surplus $P_{surplus}$ that is fed into the grid exceeds the maximum feed-in limit $P_{grid,feedIn,max}$ of 70% of the PV nominal power, the increased operation state FORCED (OS 4) is set.

If the PV surplus energy is positive and there is no curtailment, OS 3 is set to increase HP operation power. The controller works with predictions. Two hours before a predicted curtailment of at least half an hour will happen, it changes to blocking state (OS 1) to cool down the buffer storage tank so that it can absorb more heat before curtailment occurs. We use a persistence model for the forecast of electricity demand of the heating system, in which the forecast for the current day corresponds to the measurement from the previous day. The mean absolute error for the dataset we used in this prediction is 368,31 W. Prediction of the PV power and the remaining load of the building, without heating system, is already determined by the weather data and the household electricity load profile that are independent from the heating systems control and are therefore perfectly predicted.

In the real case, the energy management system only uses forecasts for PV power based on weather forecasts [41]. If there is no surplus and no grid utility lock is expected in the next two hours, the controller remains in normal operation state. In Fig. 2 the flow chart of the described control strategies shown, Fig. 3 shows the operation states as an annual heat map resulting from this control in the simulation.

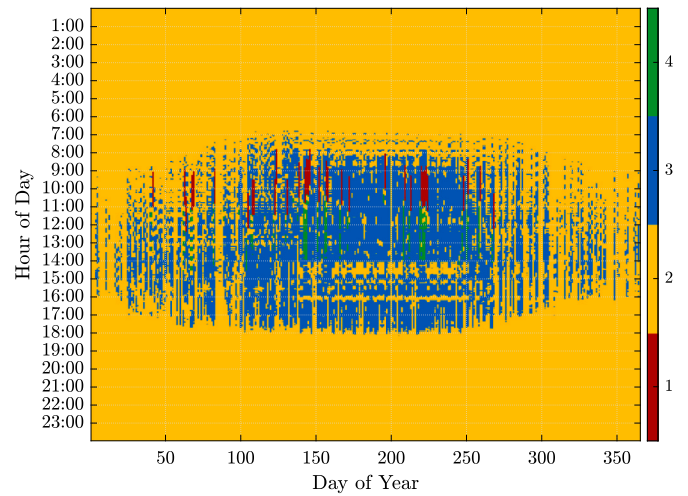


Fig. 3. SG-Ready states of S10 strategy.

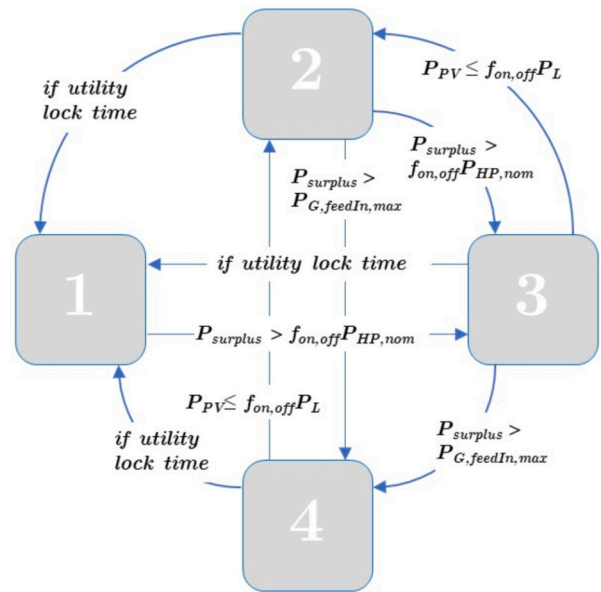


Fig. 4. SCO control algorithm flow chart (based on [7]).

6.2. Self-consumption optimized control (SCO)

The second operation strategy is based on a strategy developed by Tjaden et al. [42]. It is rule-based and designed to increase self-consumption and postpone increased HP operation during periods of increased PV surplus.

OS 1 is only reached if grid utility lock is activated. In the following, this lock is not considered because, according to information provided by the local electricity provider, it is only used to a negligible extent. However, this may vary with other electricity providers and certainly in the near future.

If the generated PV power P_{PV} is less than or equal to the current electrical household load demand P_L multiplied by the factor $f_{on,off}$, the controller changes to OS 2. With the characteristic values of the simulated PV system and the HP, Tjaden recommends a factor $f_{on,off}$ of 70%.

If the grid feed-in power or the excess PV power $P_{surplus}$ exceeds the rated power of the HP multiplied by $f_{on,off}$, the controller switches from OS 2 to the boosted state (OS 3) (Fig. 4). As soon as $P_{surplus}$ exceeds the maximum feed-in limit of 70% of the nominal PV power and there would normally be curtailment losses, the controller switches to OS 4 to

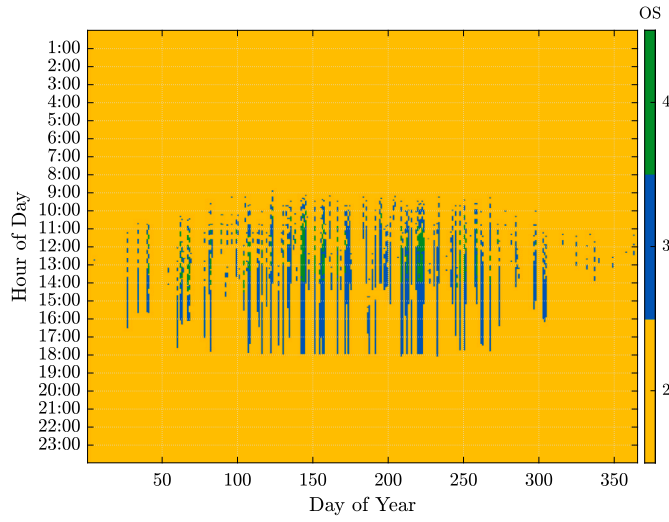


Fig. 5. SG-Ready states of SCO strategy (based on [7]).

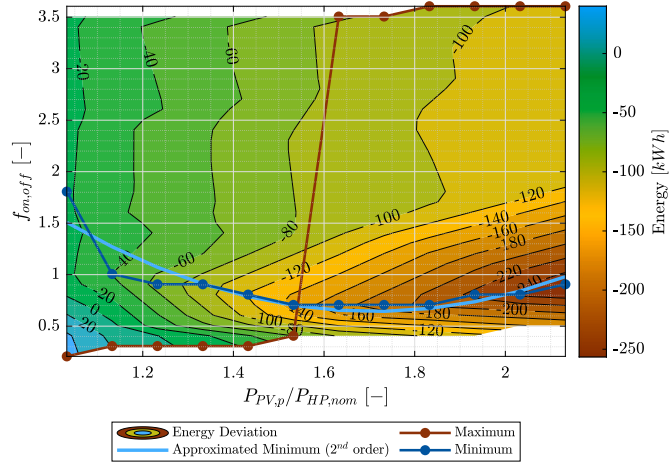


Fig. 6. Threshold factor $f_{on,off,SFH15}$ subject to ratio of PV peak power and nominal electrical power of the HP and resulting energy deviation compared to reference system for SFH 15. (For interpretation of the colors in the figure(s), the reader is referred to the web version of this article.)

increase self-consumption. Fig. 5 shows the resulting operation states, with OS 1, as already explained, not being used in the simulation. Beside the recommended values for $f_{on,off}$ by Tjaden, we examined the effect of various values of the $f_{on,off}$ on the grid demand energy for considered solar HP systems and SFH classes.

As can be seen in Figs. 6 to 8, there exists minimum values of the grid demand energy for each value of the ratio of PV peak power $P_{PV,p}$ and nominal HP power $P_{HP,nom}$ which is shown in dark blue line. With these minimal point a second order polynomial has been fitted for each SFH class and is given in equations (1d).

$$f_{on,off,SFH15} = 1.886x^2 - 6.447x + 6.153 \quad (1a)$$

$$f_{on,off,SFH45} = 2.835x^2 - 10.052x + 9.535 \quad (1b)$$

$$f_{on,off,SFH100} = -0.115x^2 - 1.392x + 4.283 \quad (1c)$$

$$\text{where } x = \frac{P_{PV,p}}{P_{HP,nom}} \quad (1d)$$

Based on these switching points, the effect in the operation strategy SCO_{opt} was considered according to the flow chart in Fig. 4 on the systems under consideration and the RRA.

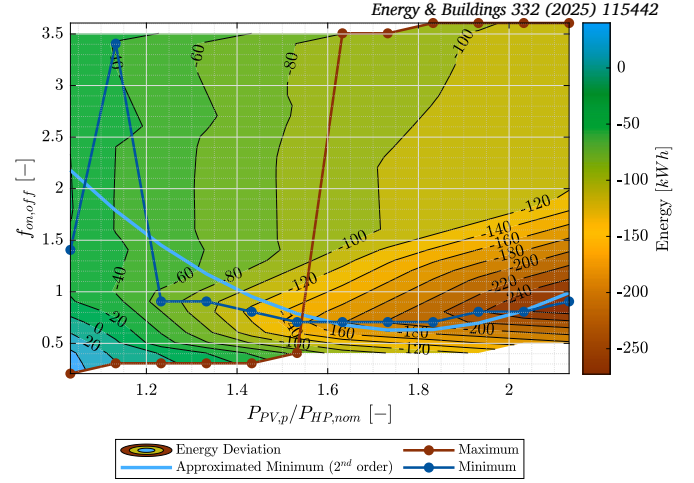


Fig. 7. Threshold factor $f_{on,off,SFH45}$ subject to ratio of PV peak power and nominal electrical power of the HP and resulting energy deviation compared to reference system for SFH 45.

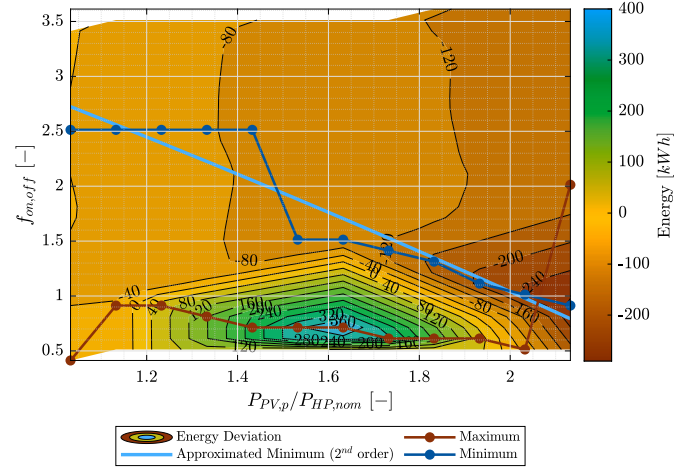


Fig. 8. Threshold factor $f_{on,off,SFH100}$ subject to ratio of PV peak power and nominal electrical power of the HP and resulting energy deviation compared to reference system for SFH 100.

6.3. Standard load profile based control (SLP)

The goal in developing this strategy was to generate a control signal based on a standard load profile (SLP). A SLP from 1996/1997 proposed by the German Association of Energy and Water Industries (BDEW) [43] for a household (category H0) is used. Three different calculation methods were used. The first method (SLP1) is based on the absolute deviation from the average daily course of the year. Table 4 shows the calculation of the limits described in the following. Based on the limit values determined in this way within the average course of the day, fixed times for one day over the entire year are obtained.

First, a daily profile averaged over a year is created and the deviation of the demand at time t from the average daily demand is determined, i.e. $P_t - \bar{P}$. The lower limit for OS 4 is the maximum negative deviation from the daily average power \bar{P} .

The upper limit for OS 4 results from the mean value of the sum of the mean negative load and the maximum negative deviation.

The mean value of the mean positive deviation and the mean negative deviation form the upper limit and the lower limit of normal state (OS 2), each with the sign reversed. This also determines the lower limit of OS 1. The upper limit of OS 1 is the maximum positive deviation.

The profile determined in this way is used for every day and does not change over the year. Fig. 9 shows the course of the day averaged over

Table 4
Range limits of *SLP1*.

SG-Ready OS	from (A)	to (B)
1	$\frac{P_{\text{min}} + P_{\text{min}}}{2} = A1$	$\max(P_i + \bar{P}) = B1$
2	$\frac{P_{\text{min}} + P_{\text{min}}}{2} = A2$	$A1 = B2$
3	$\frac{P_{\text{min}} + \min(P_i + \bar{P})}{2} = A3$	$A2 = B3$
4	$\min(P_i + \bar{P})$	$A3 = B4$

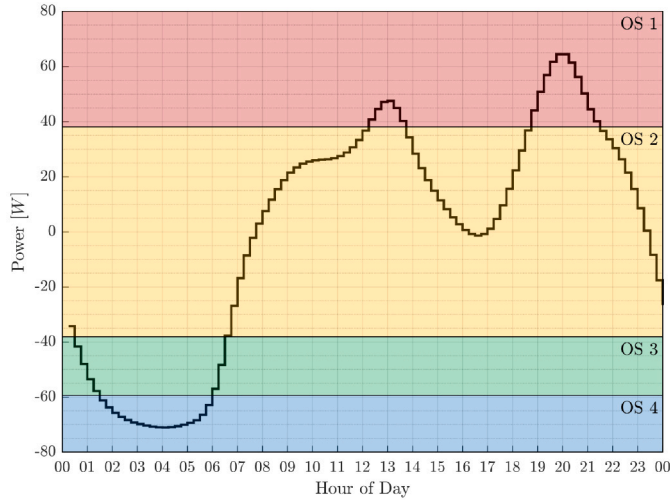


Fig. 9. Daily deviation from mean value Standard Load Profile and corresponding SG-Ready states (based on [7]).

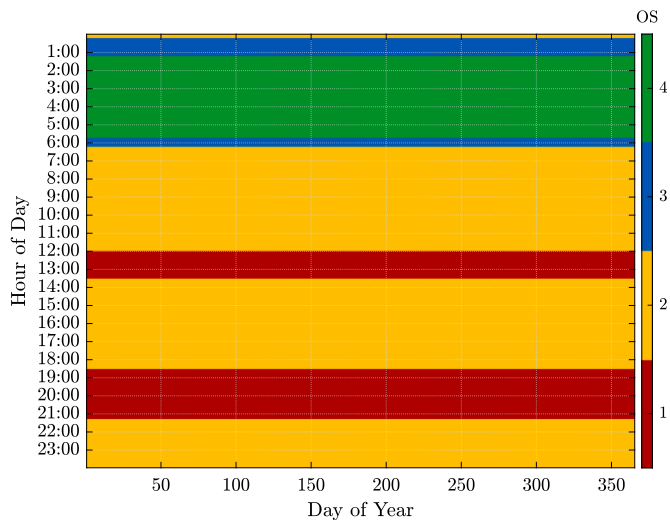


Fig. 10. SG-Ready states of *SLP1* strategy (based on [7]).

the year with the calculated limits. Fig. 10 shows the resulting profile of the operation states.

Operation strategy (*SLP2*) is also based on the BDEW standard load profile. However, the percentage deviation of the average quarter hour value is considered instead of the absolute one. The lower 10% of the load values are assigned to OS 4, the upper 15% to OS 1. Halfway between the upper limit of OS 4 and the lower limit of OS 1 is the limit of OS 2 and OS 3, which increases the value range of OS 3 compared to the previous strategy (Fig. 11).

Operation strategy (*SLP3*) corresponds to the basic principle of the previous strategy *SLP2*. However, individual days are divided into day types, i.e. workday, saturday and sunday (or public holiday).

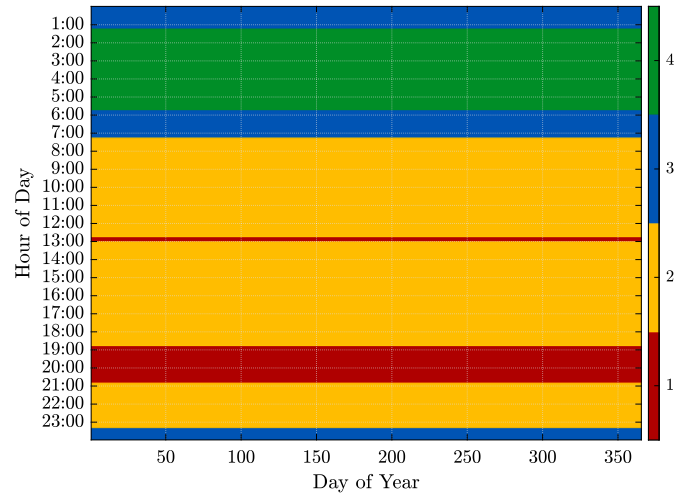


Fig. 11. SG-Ready states of *SLP2* strategy.

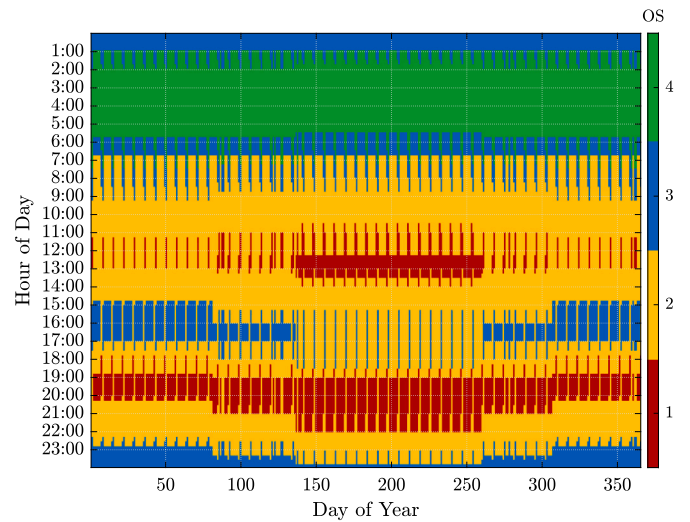


Fig. 12. SG-Ready states of *SLP3* strategy.

For further differentiation, the type days are subdivided into summer, winter and transitional periods. The division of the days was chosen to respond to the different solar radiation due to the season and the different consumption profiles depending on the day of the week. For each type day, the limits are calculated according to the same principle as the previous strategy, i.e. using the percentage deviation from the quarter-hour value of the averaged type day course. Fig. 12 shows the profile generated by this controller.

6.4. Rule-based timer control (RBTC)

These operation strategies are rule-based and follow fixed times of day.

The first strategy (*RBTC1*) is based on the HP tariff of a local DGO. In order to relieve the power grid at feed-in peak times, the utility company is permitted to switch off the HP at certain times. In return, the consumer gets a cheaper electricity tariff. This tariff is divided into day and night tariffs. The more expensive electricity price applies from 6 a.m. to 9 p.m., as demand is high during this period. The cheaper night rate applies between 9 p.m. and 6 a.m. It is therefore favorable for the consumer to operate the HP in normal operation (OS 2) during the day and to set the increased OS 3 during the night tariff. In this way, the buffer storage tank can be charged overnight. However, the utility lock

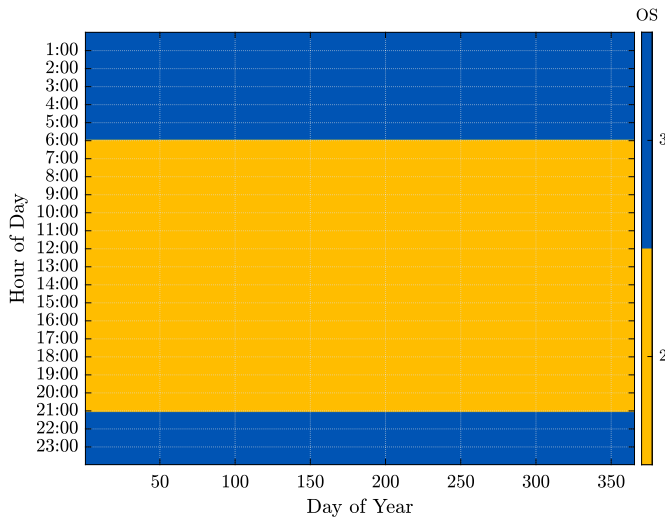


Fig. 13. SG-Ready states of *RBTC1* strategy.

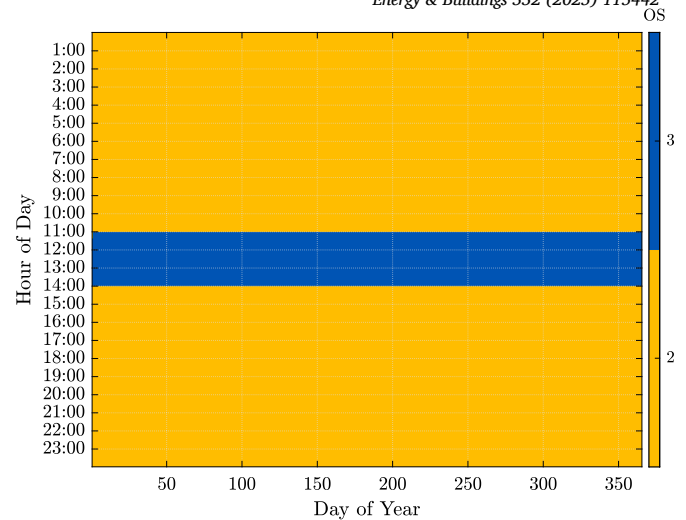


Fig. 15. SG-Ready states of *RBTC3* strategy.

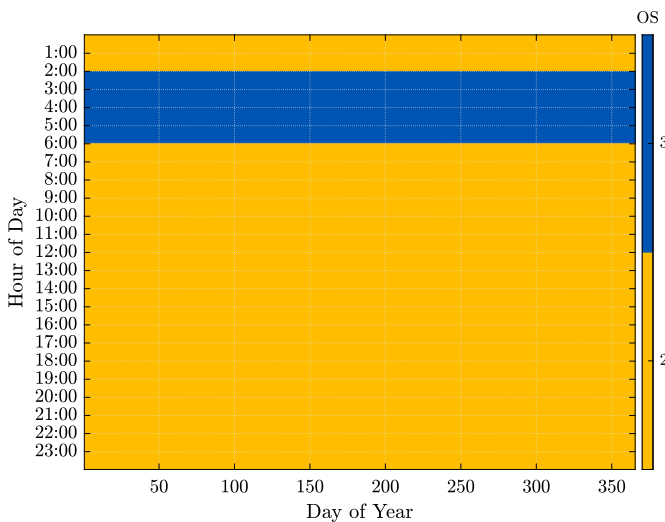


Fig. 14. SG-Ready states of *RBTC2* strategy.

is not used here because, as already explained, it is only used very rarely. Fig. 13 shows the control profile that results from these assumptions.

The next operation strategy (*RBTC2*) was developed by Fischer et al. [44] and, like the *RBTC1* control, attempts to increase or decrease HP operation at specific times. In the authors' work, the hysteresis for the storage tank temperature is increased by 5 K at times when operation should be avoided and decreased by 5 K at favorable times. Since Fischer did not use an HP with SG-Ready, the strategy must be adjusted somewhat. In times of low electricity prices, the hysteresis is to be lowered by 5 K. In our case, this is to be done by setting the boosted state (OS 3). According to Fischer, this is the case between 2 a.m. and 6 a.m. To determine this, he averaged and zoned one year's EEX day-ahead spot prices.

In times with medium electricity prices, OS 2 is set. In times when a high electricity price is expected, the hysteresis at Fischer is increased by 5 K to avoid increased operation. However, there is no operation state with weakened HP operation besides OS 2, except for OS 1. But this is a shutdown command and therefore is not desired. For this reason, normal state (OS 2) is also set in this case. So, only OS 2 and OS 3 are used in this operation strategy. Fig. 14 shows the profile that follows from this and switches at the same time every day.

The third strategy (*RBTC3*) is similar in operation to the previously mentioned strategy.

However, Fischer et al. [44] did not base this version on the level of electricity prices, but on the strength of solar radiation.

In times of highest irradiation the hysteresis should be lowered. According to Fischer et al., this is the case between 11 a.m. and 2 p.m. For our observation, the boost state (OS 3) is set during this time.

In times of low irradiation the hysteresis should be increased. Unfortunately, this cannot be realized with the SG-Ready states, which is why (as with *SLP2*) OS 2 is set. At all other times the HP also runs in OS 2. This control is only activated when the outdoor temperature of the house is above 10°C. Below this limit, normal state (OS 2) remains set. In Fig. 15 it can be seen well that the OS 3 is switched on mainly in summer.

6.5. Price and rule-based control dependent on day-ahead prices (*PRBC*)

For this rule-based operation strategy, the day-ahead prices of Germany/Austria/Luxembourg for the year 2016 are evaluated. Day-ahead trading is the trading of electricity for the following day, which is traded on EPEX Spot, a spot market of the European Power Exchange. Day-ahead trading is possible until 12 noon of the previous day. From then on, intraday trading begins. Buying electricity for the future gives the buyer a certain degree of planning certainty. The closer the time of the agreed electricity delivery, the sooner it can be estimated how high the actual demand will be. Surpluses and shortfalls should be kept as low as possible. Even though trading on power exchanges accounts for only about 20% of the total trading volume, exchange prices are considered important indicators of wholesale prices [45]. The one-year data set used is from the entsoe Transparency Platform [46]. It was cleaned using methods used by Rheinberger et al. [47] and interpolated to 15-minute values. The algorithm determines the maximum and minimum day-ahead prices separately for each day. In principle, this is a perfect prediction. The range between the maximum and the minimum is divided and assigned to the four operation states. The division is arbitrary. For this work, four different variants with different limits were simulated and evaluated. In variant 1, for example, the lower 5% of the day-ahead prices on the corresponding day are assigned to OS 4. Above the 5% limit up to the 10% limit is the range assigned to OS 3. Starting from this limit up to 85% is the range for OS 2. The upper 15% belongs to OS 1. After calculating the limits, the day-ahead price at corresponding date and time is retrieved and compared with the calculated limits of the current day. Depending on which limits the price lies between, the corresponding operation condition of the HP is set. The described methodology was then applied to the annual profile with other limits. All variants can be seen in Table 5 and in Fig. 16 to Fig. 19.

Table 5
Range limits of *PRBC*.

SG-Ready State	Variants 1	Variants 2	Variants 3	Variants 4
1	85 - 100%	90 - 100%	90 - 100%	70 - 100%
2	10 - 85%	25 - 90%	60 - 90%	50 - 70%
3	5 - 10%	5 - 25%	10 - 60%	30 - 50%
4	0 - 5%	0 - 5%	0 - 10%	0 - 30%

0%: Daily Minimum of Day-Ahead Price.
100%: Daily Maximum of Day-Ahead Price.

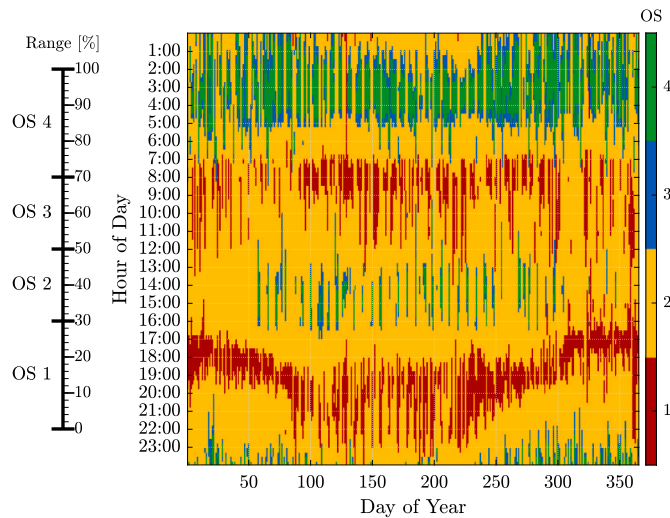


Fig. 16. SG-Ready states of *PRBC1* control strategy.

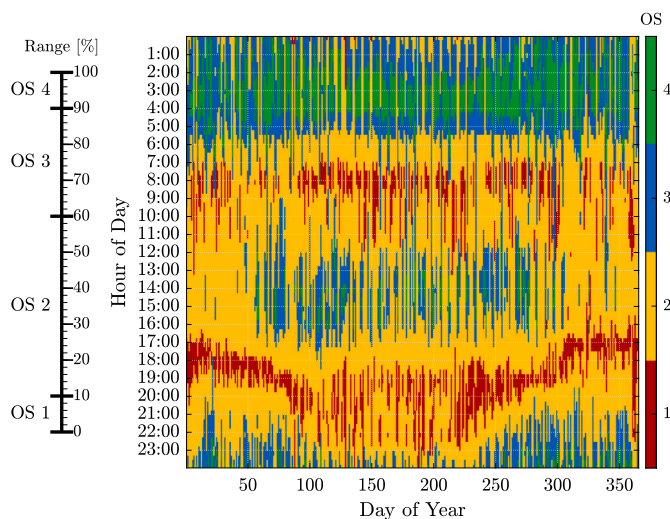


Fig. 17. SG-Ready states of *PRBC2* control strategy.

The aim of this operation strategy is to keep costs low for the end user. In times when the electricity price is high, the HP operation is reduced and in times of low electricity prices the operation is increased, and the buffer storage tank is charged.

Fig. 16 shows the operation states of *PRBC1*. On the left side of the scale, the simulation is based on the division of the range of day-ahead electricity prices to which the operation states are assigned. Thus, the range of OS 4 covers the lower 5% of prices on the corresponding day; the range from 5% to 10% is assigned to OS 3, etc. In this variant, OS 2 is clearly the dominant one, as can be seen from the yellow coloring. At 8 a.m., as well as around 6 p.m., it can be seen from the mostly red coloring that the price of electricity is most expensive at this time.

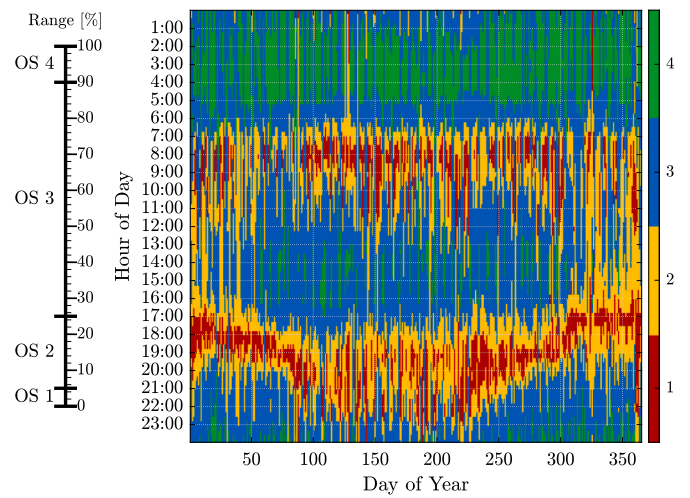


Fig. 18. SG-Ready states of *PRBC3* control strategy.

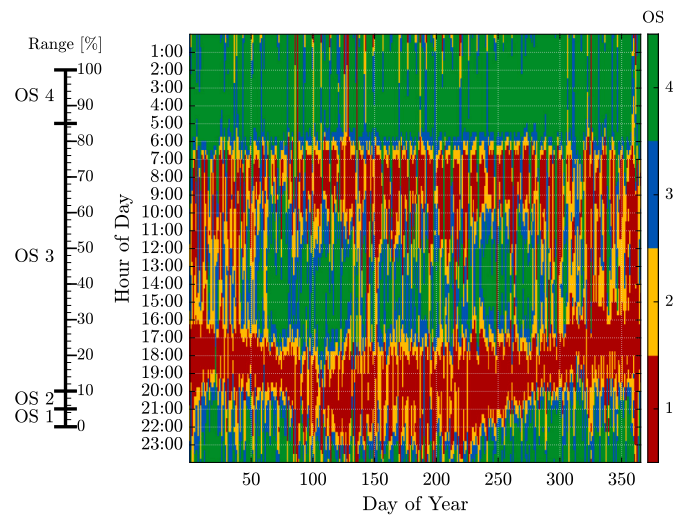


Fig. 19. SG-Ready states of *PRBC4* control strategy.

In summer, this shifts to the evening hours. In the morning, when the electricity price is low, the buffer storage is charged by switching on the increased operation. Operation State 3 is set relatively rarely. In the second variant, the increased blue content in Fig. 17 clearly shows that the area of OS 3 has been enlarged somewhat. However, OS 2 is still the dominant operation state. Here, too, the high-price periods, i.e., around 8 a.m. and 6 p.m., are clearly visible.

In variant 3, OS 3 is assigned the largest area, as can be seen in Fig. 18. This can also be seen from the dominant blue color. Only at the high price periods OS 1 and OS 2 are mostly set. Otherwise, the two operation states are rarely used. OS 4 continues to be used for the most part only in the very early morning hours. In the fourth variant, the ranges of OS 1 and OS 4 are the dominant ones, as can be seen in Fig. 19. During the high price periods, mainly OS 1 is set and during the other periods mainly OS 4 is set. With OS 2 and OS 3, on the other hand, the HP is rarely actuated.

7. Evaluation indicators

When evaluating the simulation regarding the grid serviceability and plant operator serviceability of the different operation strategies, various aspects have to be considered.

7.1. Self-consumption rate

The self-consumption rate (*SCR*) is the proportion of self-used energy, either through direct consumption ($E_{PV2Load}$) or through storage in the battery storage system ($E_{PV2Batt}$), in relation to the PV energy generated (E_{PV}). A self-consumption rate of 100% would mean that all of the PV energy is used and nothing is fed into the grid. This is also worthwhile financially, as the feed-in tariff for electricity fed into the grid is lower than the purchase price.

$$SCR = \frac{E_{PV2Load} + E_{PV2Batt}}{E_{PV}} \cdot 100\% \quad (2)$$

7.2. Self-sufficiency rate

The degree of self-sufficiency (*SSR*) provides information on the proportion of self-generated energy, either through direct consumption of PV energy ($E_{PV2Load}$) or from battery storage ($E_{Batt2Load}$), in relation to the total energy requirement E_{Load} . A degree of self-sufficiency of 100% would be ideal, as this means that the entire energy requirement is covered by self-generated energy.

$$SSR = \frac{E_{PV2Load} + E_{Batt2Load}}{E_{Load}} \cdot 100\% \quad (3)$$

7.3. Seasonal performance factor

The seasonal performance factor $SPF_{SH P+,pen}$ gives the ratio of the useful heat consumed for space heating and hot water production and the electrical consumption of the whole heating system [48]. In case of violation of the comfort criteria defined by the Task 44 of the SHC program (hot water tap temperature and room temperature of the building), so-called penalty functions are applied [49]. They are added to the electrical load of the heating system and represent the missing heating energy needed to meet the comfort criteria. The electrical load of the heating system includes the power of the HP, the HP control, the HP storage charging pump, the DHW pump, the heating circulation pump and additional controller.

$$SPF_{SH P+,pen} = \frac{Q_{DHW} + Q_{SH}}{E_{el,SH P+,pen}} \quad (4)$$

7.4. Fractional CO₂ emission savings

Fractional CO₂ emission savings f_{sav,CO_2} is a measure of how many CO₂ emissions can be saved compared to a conventional heating system and is defined (Equ. (5)).

$$f_{sav,CO_2} = \frac{\sum_{i=1}^{n_{es}} (E_{fe,i} GW P_i)_{HP}}{\sum_{i=1}^{n_{es}} (E_{fe,i} GW P_i)_{ref}} \quad (5)$$

$$= 1 - \frac{(E_{el,SH P+,pen} GW P_{el})_{HP}}{\frac{Q_{DHW,ref} + Q_{SH,ref}}{n_{ref}} GW P_{gas} + E_{el,ref} GW P_{el}}$$

where	$E_{fe,i}$	[kWh]	final energy consumed by energy source i
	$GW P_i$	$[\frac{kgCO_2eq}{kWh}]$	global warming potential for energy source i
	$E_{el,SH P+,pen}$	[kWh]	total electrical consumption of the heating system incl. penalties
	$Q_{DHW,ref}$	[kWh]	preset consumed heat quantity for hot water preparation

$Q_{SH,ref}$	[kWh]	Energy & Buildings 332 (2025) 115442 Preset consumed heat quantity for space heating
η_{ref}	[-]	efficiency of the reference gas heating system
n_{es}	[-]	number of energy sources

In this case, a gas heating system including electrical controls and hot water circulation pumps [48] was used as the conventional heating system. The electricity consumption of the reference heating system $E_{el,ref}$ in one year is 204 kWh. The efficiency factor η_{ref} is the overall efficiency of the reference system and is assumed to be 0.9. The heat demand in the whole year for space heating $Q_{SH,ref}$ and DHW preparation $Q_{DHW,ref}$, are already given by the building as 6,476 kWh/a for space heating and 2,076 kWh/a for domestic hot water preparation respectively. The Global Warming Potential (*GW P*) of the respective final energy carrier defines its relative global warming potential with respect to CO₂ emissions and is 0.5210 kg CO₂eq./kWh ($GW P_{el}$) and 0.307 kg CO₂eq./kWh ($GW P_{gas}$) respectively. For the electrical load of the heating system $E_{el,SH P+,pen}$, electrical power consumption of the HP, HP control, HP storage tank charging pump, the DHW pump, the SH circulation pump as well as additional controller including the previously mentioned penalty function are included in the violation of the comfort criteria.

7.5. Relative Import Bill

The Relative Import Bill (*RIB*) is a quantity that considers load shifting from high price periods to low price periods [50]. The quantity looks at the reduction in the electricity bill for variable price tariffs. For the evaluation, it is assumed that there is a variable-price tariff for each strategy considered. The electricity bill is calculated by multiplying the grid purchase at time t by the corresponding day-ahead electricity price and adding it all up. The possible reduction in the electricity bill is this sum minus the minimum possible electricity bill. This is the sum of the grid purchase at time t multiplied by the minimum day-ahead price on the corresponding day. The difference between the electricity bill and the minimum possible electricity bill is set in relation to the difference between the maximum possible bill and the minimum possible bill. The maximum possible bill is calculated equivalent to the minimum with the daily maximum price.

Desirable for the *RIB* would be a value as close to zero as possible. This would mean that the electricity was purchased at the most favorable times. A favorable exchange price leads to lower electricity procurement costs for the energy suppliers and thus to a more favorable end customer price. However, this relationship is not linear, since the EEG surcharge increases as the exchange price falls [51]. In addition, other factors play a role in the cost calculation of the end customer price. The size is thus relevant for the plant operator, who wants to purchase the electricity at the lowest possible prices. It is also relevant for the grid operator. For this purpose, it is assumed that a high day-ahead electricity price corresponds to a high electricity demand at that time. This assumption is supported by Fig. 20 and Fig. 21. The daily curves of the day-ahead electricity price and the BDEW standard load profile averaged over the year are shown in Fig. 20 and Fig. 21 respectively. It can be seen that the trajectories are similar for mean values, and rise and fall at approximately the same times.

When the demand for electricity is high, it is beneficial to the grid to reduce the load on the grid by reducing the amount of electricity drawn from the grid.

$$RIB = \frac{\sum_{t=0}^T (E_{G,D}(t) p_{el}(t)) - \sum_{t=0}^T (E_{G,D}(t) \underline{p}_{el,d}(t))}{\sum_{t=0}^T (E_{G,D}(t) \overline{p}_{el,d}(t)) - \sum_{t=0}^T (E_{G,D}(t) \underline{p}_{el,d}(t))} \quad (6)$$

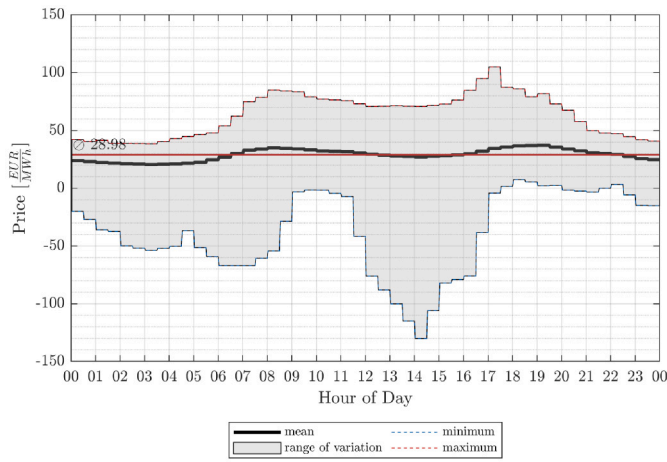


Fig. 20. Mean, maximum and minimum day-ahead electricity price of an annual dataset for one day.

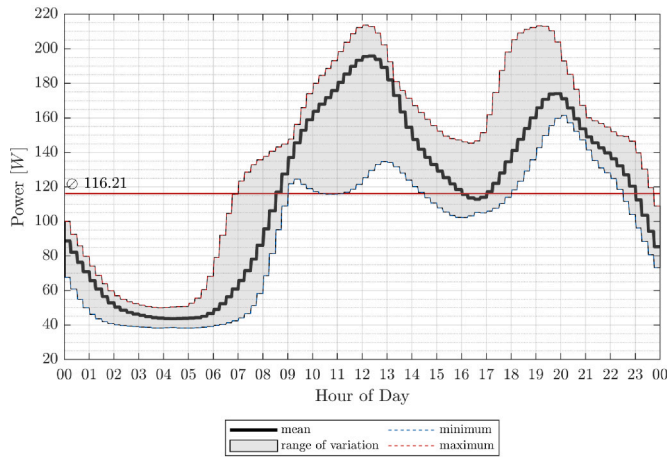


Fig. 21. Mean, maximum and minimum standard load profile of an annual dataset for one day.

where	$E_{G,D}(t)$	[kWh]	grid demand energy
	$p_{el}(t)$	$[\frac{\text{€}}{\text{kWh}}]$	day-ahead electricity price at time step t
	$\underline{p_{el,d}}(d)$	$[\frac{\text{€}}{\text{kWh}}]$	minimal day-head electricity price of day d
	$\overline{p_{el,d}}(d)$	$[\frac{\text{€}}{\text{kWh}}]$	maximal day-head electricity price of day d

7.6. Absolute Grid Support Coefficient

Absolute Grid Support Coefficient GSC_{abs} is intended to provide information on how well the end user's electricity consumption profile matches the availability of electricity [52]. It indicates whether electricity consumption tends to occur during periods when the day-ahead electricity price is greater than the average relative price or during periods when it is less. This allows an assessment of the grid impact of a building from the utility's perspective. For a flexible load such as a HP, a GSC_{abs} of 0.9 means that, on average, electricity is consumed when the day-ahead price assumes 90% of its mean value during the evaluation period. A low GSC_{abs} is desired, as this means that electricity is mainly consumed when the electricity price is low, or when the demand for electricity is low. This makes sense for both the end consumer and the utility.

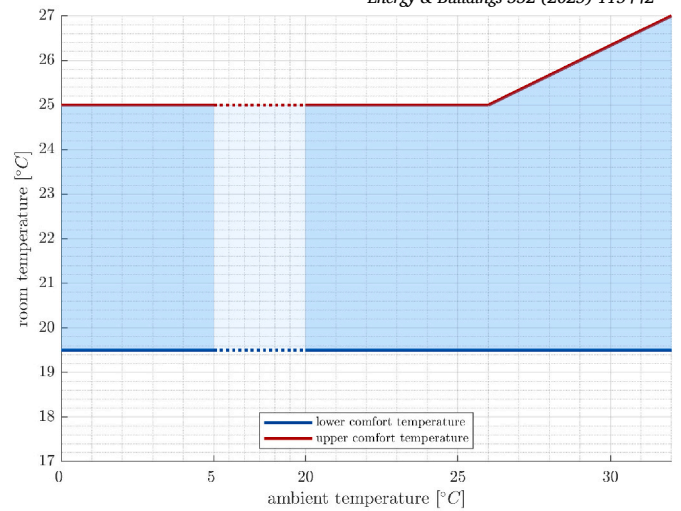


Fig. 22. Thermal comfort range.

$$GSC_{abs} = \frac{\sum_{t=0}^T (E_L(t)p_{el}(t))}{\sum_{t=0}^T (E_L(t)) \frac{1}{T} \sum_{t=0}^T p_{el}(t)} \quad (7)$$

where $E_L(t)$ [kWh] total energy consumed by household load at time step t
 $p_{el}(t)$ $[\frac{\text{€}}{\text{kWh}}]$ day-ahead electricity price at time step t

7.7. Time of thermal discomfort

The total time $t_{T<}$ during which the comfort criteria are violated is of great importance to the home user. As regulated in Task 44, the room temperature must not fall below 19.5°C [53]. The upper limit for the temperature can be found in DIN Standard 1946 Part 2 [54]. Up to a maximum outside temperature of 26°C, the room temperature must not exceed 25°C. If the outdoor temperature is above 26°C, the room temperature may also be higher, corresponding to the red marked line in Fig. 22.

When evaluating this evaluation parameter, it was noticed that the time in which the room temperature exceeds the upper limit of the comfort range is almost exactly the same for all strategies considered, namely 928.95 hours. This value is many times higher than the time during which the temperature falls below the upper limit. The high room temperature is due to high outside temperatures. The simulated building needs a relatively long time to cool down once the temperature has increased, since no active room cooling is installed. For this reason, the quantity $t_{T<}$ is introduced, which only considers the undershoots of the comfort range.

7.8. Number of heat pump starts

The number of HP starts n_{starts} has an impact on both the system owner and the grid operator. From the grid operator's point of view, the reference power peaks associated with compressor starts have a negative impact on the stability of the electricity grid. In their laboratory tests, Akmal et al. [55] investigated the starting behavior of HPs and observed that the starting current with soft start of the compressor motor is around twice as high as in normal operation. Without soft starters, current peaks are typically observed, which are around 4 to 7 times higher than in full load operation. The compressor motor accounts for around 90% of the electricity demand of the entire HP system and therefore dominates the influence on the purchasing power from the grid. From a system owner point of view, a low number of HP cycles is preferred

as unnecessary on/off cycling reduces the lifetime of the compressor [56]. In addition to on/off-controlled HPs, frequency-controlled, also known as inverter-driven, HPs, have been establishing themselves for some years now. Research indicates that inverter-driven HPs generally outperform on/off HPs in terms of energy efficiency and seasonal performance. Schio and Ballerini [57] found that inverter-driven HPs achieved at least 10% higher *SPF* compared to on/off models. Apart from this, inverter-driven HPs require less starting power than fixed-speed types [58]. Nevertheless, the focus in this paper is on the on/off-controlled HPs.

8. Simulation framework

8.1. Software and system model parameters

The simulation of the building and all system components is done via the TRNSYS simulation environment [59]. The residential energy system model including building, solar, and HP system is based on the work presented in [10–12] using models of the SHP-SIMLIB [60]. A detailed description of the model and discussion of solar heat pump systems can be found in [28]. The main components have been listed in Table 6.

Table 6
System model parameters.

Component	TRNSYS Type	Description	Value
battery system	47 [59]	capacity	5.5 kWh
		efficiency	0.94%
PV system	835 [63]	peak power	2.45 kWp
		inverter efficiency	0.96%
HP	401 [64]	el. nom. power (A7/W35)	1.8 kW
		therm. nom. power (A7/W35)	7.6 kW
storage tank	340 [65]	Volume	1 m ³
building	56 [59]	heating area	140 m ²

Building Controls Virtual Test Bed (BCVTB) [61] acts as a middleware between TRNSYS and MATLAB [62]. Type 6666, provided by the TRNSYS vendor Transsolar, enables TRNSYS to send and receive data to and from MATLAB. In MATLAB a template script provided by BCVTB is used to establish the socket communication. MATLAB, where the control strategies for the heat pump are implemented, transfers the control signal in each simulation step via BCVTB to TRNSYS and receives input data needed for the control (Fig. 23). The control signal is compatible with the SG Ready-interface of the on/off state-controlled heat pump in TRNSYS.

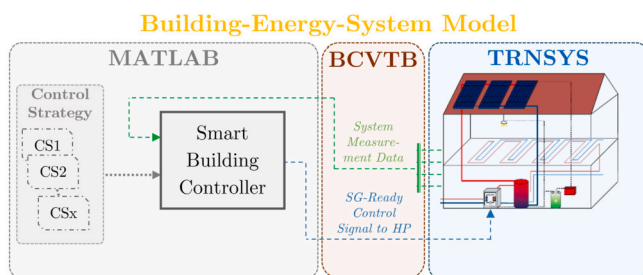


Fig. 23. Simulation framework (based on [7]).

8.2. Implementation of SG-Ready operation states

The BWP has defined the requirements for controllability in the SG-Ready Label regulations for heat pumps [19]. The specific implementation is the responsibility of the HP manufacturers and experience

Table 7
Implementation of SG-Ready states.

SG-Ready OS	Description
1 (OFF)	OFF state: The HP is switched-off
2 (NORMAL)	The HP runs in normal state. At a temperature of 53 °C in the DHW zone of the storage tank the HP switches on to supply this zone with heat until it reaches 55 °C. In the SH zone of the tank, the HP supplies heat when the temperature difference between the SH zone sensor and the setpoint is less than 0 K until the difference exceeds 3 K. The setpoint is calculated using a weather-compensated flow temperature control, which depends mainly on the outdoor temperature and the design heat load of the building and location.
3 (BOOST)	The HP controller is recommended to switch-on: The storage tank setpoint temperatures for DHW and SH zone, both are increased by 5 K.
4 (FORCED)	Actuation signal to the HP controller. Both setpoint temperatures are increased to the setpoint of the DHW zone plus 5 K.

has shown that it is not published in detail. Depending on the manufacturer, setpoint increases of the hot water and heating water temperature can be up to 50 K [66], whereby the achievability of the temperature levels depends on further safety criteria and the technical performance of the heat pump. We refer to the manufacturer’s recommendations when selecting the temperature increase of 5 K [67]. Fischer et al. [22] also used this value in their studies.

The corresponding implementation of the four SG-Ready Operation States depends on the hot water storage tank temperature and is summarized in Table 7.

In NORMAL operation state, the switching points are between 53°C and 55°C in the domestic hot water area of the buffer tank. A weather-compensated characteristic curve for the flow temperature is used for space heating, with switching points at 0 K and 3 K.

In BOOST state, the setpoint temperatures are increased by 5 K and in FORCED state, the setpoint temperature for the room heating is also raised to that of the domestic hot water temperature in order to force a definitive HP start.

9. Results

9.1. Single family households

This section discusses the individual results of the six different building types for the operation strategies and the evaluation indicators described above. These are shown in Fig. 24 and Fig. 25 respectively. The key indicators *SSR* and *SCR* (cf. Fig. 24) are only relevant for buildings with a PV system, as they consider the PV energy generated. These values are zero if no PV system is installed and are therefore not considered in the two figures for such systems.

When looking at the *SSR*, it can be seen that it increases slightly with a better renovation status. For the reference case, for example, this results in a value of approx. 33% for PV-SFH015 and 29.5% for PV-SFH100. It can be seen that the values for PV-SFH15 for all operation strategies are between approx. 30.3% and 35.2% and for PV-SFH100 between approx. 31.4% and 23.8%. The spread between the building renovation levels is (from PV-SFH015 to PV-SFH100) between 2.7% (*SLP1*) and 6.6% (*PRBC4*), with the mean value being 3.6%. The maximum *SSR* is 35.2% for PV-SHP015 for the *SCO* and *SCO_{opt}* operation strategy, with *SCO_{opt}* for PV-SHF100 performing slightly better at 31.4% than *SCO* at 31.2%. The minimum *SSR* is 23.8% for *PRBC4* and PV-SFH100.

If you look at the *SCR*, you can see that it does not show a clear dependency on the renovation status. For the reference case, for example, there is a value of approx. 91.9% for PV-SFH015 and 92.4%

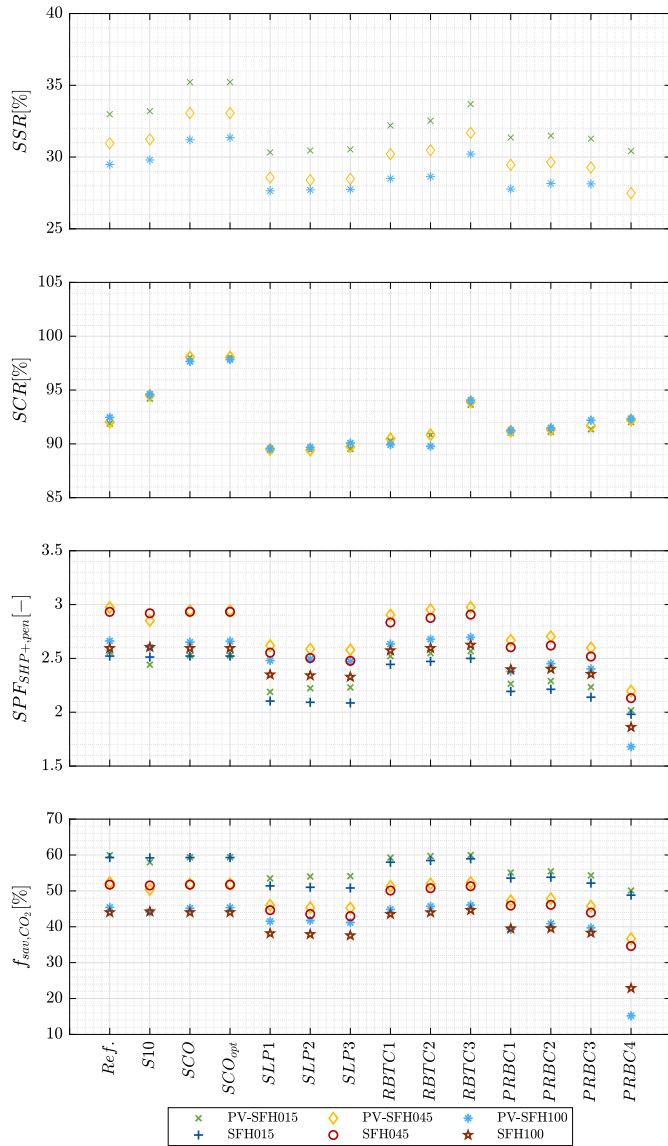


Fig. 24. Evaluation results of Single Household, Part 1.

for PV-SFH100. For SCO_{opt} , on the other hand, it drops from 98% for PV-SFH015 to 97.6% for PV-SFH100. The values for PV-SFH015 are between approx. 89.4% and 98% for all operation strategies and between approx. 89.5% and 97.8% for PV-SFH100. The maximum SCR is 98% for PV-SFH015 with the operation strategies SCO and SCO_{opt} , with SCO_{opt} for PV-SFH100 performing slightly better at 97.8% than SCO at 97.6%. The minimum SCR is 89.4% for $SLP2$ and PV-SFH15.

When looking at the $SPF_{SHP+,pen}$, the maximum is consistently found for PV-SFH045 and SFH045, whereby the values for buildings with a PV system are slightly better except for the operation strategy $S10$. With the exception of the $S10$ operation strategy, buildings with PV systems achieve better results for all building types and for SFH100 in the $PRBC1$ and $PRBC4$ operation strategies. The maximum value of almost 3.0 is achieved for PV-SFH045 with $PRBC3$ and the minimum value of 1.7 for PV-SFH100 with $PRBC4$. This shows that operation strategies that maximize self-consumption do not directly lead to a higher SPF . For buildings without a PV system, the minimum value is almost 1.9 for SFH100 with $PRBC4$ and the maximum value is 2.9 for SFH045 with the operation strategies SCO , SCO_{opt} and the reference operation strategy.

Fractional CO_2 emission savings f_{sav,CO_2} shows a clear dependence on the building renovation status. The savings decrease with a poorer

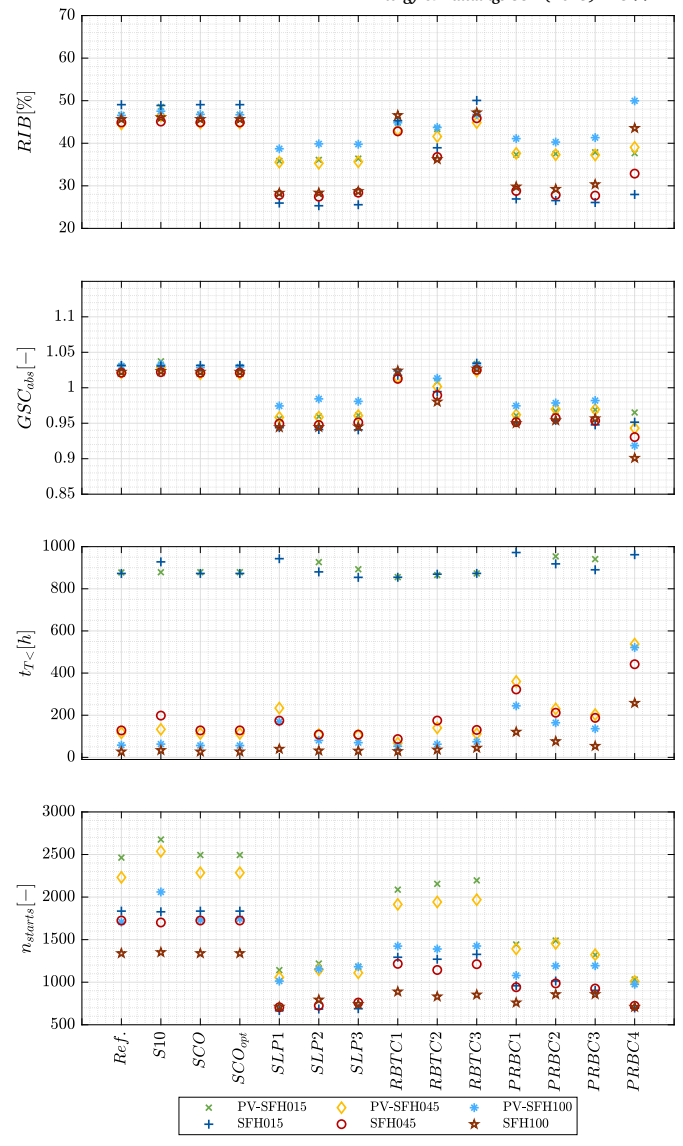


Fig. 25. Evaluation results of Single Household, Part 2.

renovation status. Here too, the values are predominantly better for systems with a PV system than without. The only exceptions here are the $S10$ operation strategy and $PRBC1$ as well as $PRBC4$ for SFH100, which is similar to $SPF_{SHP+,pen}$. The minimum value for systems with a PV system is 15.1% (PV-SFH100) and is achieved with $PRBC4$, the maximum value of just under 60% with $PRBC3$ (PV-SFH015). For systems without a PV system, the savings are between 22.8% (SFH100, $PRBC4$) and 59.3% (SFH015, $Ref/SCO/SCO_{opt}$).

The RIB, on the other hand, shows no clear dependency on the building renovation status. While the best (minimum) value for buildings with a PV system is PV-SFH045 (exception for $PRBC1$ and $PRBC1$, here PV-SFH015), for systems without a PV system it is predominantly SFH015 and SFH045 (exception for $PRBC2$, here SFH100). The minimum value for systems with a PV system is 35.3% (PV-SFH045) and is achieved with $SLP2$, the maximum value of just under 50% with $PRBC4$ (PV-SFH100). For systems without a PV system, the values are between 25.8% (SFH015, $SLP2$) and 50% (SFH015, $RBC3$). It can be seen here that the HP can flexibly follow the control signal, whereby systems without a PV system predominantly achieve better results.

For GSC_{obs} , too, no clear tendencies can be recognized with regard to the degree of building renovation; only for buildings with a PV system are the better values predominantly found for PV-SFH045. The tenden-

cies are similar to *RIB*, as can be seen in Fig. 25, whereby systems without PV systems predominantly achieve better results. The minimum value for systems with a PV system is around 0.92 (PV-SFH100) and is achieved with *PRBC4*, the maximum value of just under 1.04 with *S10* (PV-SFH015). For systems without a PV system, the values are between 0.9 (SFH100, *PRBC4*) and 1.03 (SFH015, *RBC3*).

When looking at the times when the temperature falls below the thermal comfort limit of 19.5°C, $t_{T<}$, there is a gradient towards the building types with a lower renovation status, i.e. the times are much lower for (PV-)SFH100 than for (PV-)SFH015 and (PV-)SFH045. One possible explanation for this is the presence of forced ventilation in the (PV-)SFH015 standard in accordance with the specifications for the building model [39] and a heating controller that is probably not optimally designed. Both the mean maximum deviations across all operation strategies of approx. 1.8 K and the mean frequency of 90.8% for falling below the comfort temperature in the interval 0 to 0.05 K for SFH015 are worse than for SFH100 (1.4 K, 99.3%). A high frequency for this interval is to be seen as positive, as the proportion of higher temperature deviations then decreases at the same time. This applies in a similar way to the buildings with PV systems. The frequency of falling below 0.05 K increases from PV-SFH015 with 90.5% to 98.1% for PV-SFH045 and 98.6% for PV-SFH100. In contrast, PV-SFH015 and PV-SFH100 are roughly on a par at 1.8 K for the maximum temperature undershoot averaged over all operation strategies, whereas PV-SFH045 is at 1.1 K. The poor values for the OS *PRBC1* to *PRBC4* are particularly noteworthy. Here, maximum temperature undershoots occur with PV-SFH100 between 2.6 K (*PRBC1*) and 6.9 K (*PRBC4*). The situation is similar for buildings without a PV system. Here, the worst values are also at *PRBC4* with 6.4 K and *PRBC2* with 2.6 K. As described in Section 6.5, the switching limits between the SG-Ready states were chosen arbitrarily based on the price curve. However, the results show that the losses in comfort are lowest for the limits selected in *PRBC3*.

The number of HP starts n_{starts} predominantly shows a behavior that increases with a better degree of renovation. For buildings without a PV system, the operation strategies form exceptions *SLP1* and *SLP2* as well as *SLP2*, *PRBC3* and *PRBC4*. For the first two, the behavior is reversed. Here, n_{starts} decreases as the renovation status improves. For the latter three, however, the highest number is SFH045. For buildings with a PV system, the exceptions are *SLP2* and *SLP3* as well as *PRBC3*. While n_{starts} decreases for the first two as the renovation status improves, the maximum for *PRBC3* is again at PV-SFH045. For all operation strategies and renovation statuses, the number of HP starts for systems with a PV system is higher than for the corresponding buildings without a PV system. The minima are 667 for SFH015 with *SLP1* and 975 for PV-SFH100 with *PRBC4* for buildings with a PV system. The maxima, on the other hand, are 1835 for SFH015 with the reference system, *SCO* and *SCO_{opt}* and 2676 with *S10* for PV-SFH015.

9.2. Representative residential area

The overall evaluation indicators for the RRA defined in Section 5 are calculated by first calculating the assessment quantities for a single building type, as discussed in previous section. In a second step the values are scaled to the RRA using Equ. (8). This means the obtained values are multiplied by the number of buildings of this type in the RRA and summed up. After that, the obtained value is divided by the total number of buildings in the RRA, so that a weighted average value of the evaluation variables for the whole area is obtained.

$$X_{RRA} = \frac{\sum_{i=1}^m X_i n_i}{\sum_{i=1}^m n_i} \quad (8)$$

where $X_{ResArea}$ is the total evaluation value of the residential area, where X represents the different evaluation values as SPF or RIB. X_i is

the evaluation value X of each building type i , that are SFH15, SFH45, SFH100 with or without PV plant. n is the number of buildings of each type i in the residential area. The following Table 9 provides an overview of how the evaluation parameters are to be classified.

In the next step, the results for each evaluation indicator were scaled within the value range for the RRA. It was taken into account that small values are better for the evaluation metrics f_{cl} , *RIB*, GSC_{abs} , $t_{T<}$ and n_{starts} and the value range was inverted for this (see Table 9). These relative values were used to calculate the mean value across all evaluation indicators for each operation strategy. This value was used to rank the operation strategies. The absolute results of the individual evaluation indicators for the RRA, the scaled values averaged across all evaluation indicators and the results of the ranking in the range 1 (best) to 14 (worst) are shown in Table 8. These are discussed below.

If you look at the *SSR*, you can see that *SCO* and *SCO_{opt}* have the best values, surprisingly followed by *RBTC3*. This underlines the fact that even a fairly simple time-controlled control system has a noticeably positive effect on the degree of self-sufficiency. The *S10* strategy is close behind, closely followed by the reference strategy. As expected, the *SLP* strategies show poor values at the same level. The worst performer is *PRBC4* with a value of 2.88. The picture is similar for *SCR* and f_{cl} . Here, however, *S10* is ahead of *RBTC3*, followed by *Ref*. The *SLP* strategies have the worst values. In terms of the annual performance factor $SPV_{SHPP+pen}$ and fractional CO_2 emission savings f_{sav,CO_2} , operation strategies *Ref*, *S10*, *EVO*, *EVO_{opt}* and *RBTC1* to *RBC3* are almost on a par, with *RBTC1* and *RBTC_{opt}* being slightly worse. This is followed by the *PRBC* strategies, followed by the *SLP* strategies. As with *SSR*, the value of 2.02, 30.56 respectively is worst for *PRBC4*.

Also *RIB* and GSC_{abs} show the same tendencies except for *PRBC4*. The values of these two ratios are best for the *SLP* and *PRBC* strategies, with the exception mentioned above. Only for GSC_{abs} is the value for *PRBC4* even better at 0.92. The operation strategies mentioned show similar values between 29.36 and 30.17, or 0.95 to 0.96. The worst results are found for *Ref*, *S10*, *EVO*, *EVO_{opt}*, *RBTC1* and *RBTC3*. These are between 45.26% and 46.44%, or 1.02 respectively.

When looking at the times of thermal discomfort, $t_{T<}$, it can be seen that *RBTC1* provides the best result with 95.26 h, followed by *SLP3* and *SLP2*. This is followed by *Ref*, *SCO* and *SCO_{opt}* with around 120 h. *S10* is on a par with *SLP1* with values around 163 h. At almost 411 h, *PRBC4* brings up the rear.

Looking at the number of HP starts per year, n_{starts} , the best value of 742 is achieved with *SLP1*, closely followed by *PRBC4* with 747. Surprisingly, the number of starts rises to over 1600 with the strategies *S10*, *SCO* and *SCO_{opt}* and are thus at the same level as the reference operation strategy.

As explained at the beginning of this section, an attempt was made to implement a uniform overall assessment for the RRA in such a way that all evaluation indicators considered are equally weighted and scaled to the value ranges that occurred in this study and included in the overall result (see Table 8, *Ranking*) that shows a compromise between system operator and grid operator-friendly behavior. This resulted in a ranking with *PRBC2* as a price signal-based operation strategy at the top, closely followed by the OSs based on standard load profile, *SLP2* in second place and *SLP1* and *SLP3* in 3rd and 4th place respectively. However, when comparing the ranking of *PRBC1* to *PRBC4* (places 1 to 14), it can be concluded that the switching thresholds must be well coordinated depending on the structure of the residential area. Self-consumption optimized OS *SCO_{opt}* in 6th and *SCO* in 7th place are in the midfield of the results. The reference strategy and the *S10* strategy are also at the bottom of the overall results. In the case of the *S10* strategy, this could be due to the poor quality of the predictions used.

10. Conclusion and outlook

In this article, a comprehensive evaluation of the effects of different operation strategies for HP systems was carried out. On the one hand,

Table 8
Evaluation results for the RRA.

Evaluation Indicator	Ref	S10	SCO	SCO _{opt}	SLP1	SLP2	SLP3	RBTC1	RBTC2	RBTC3	PRBC1	PRBC2	PRBC3	PRBC4
SSR[%]	3.35	3.38	3.57	3.57	3.11	3.1	3.11	3.26	3.28	3.43	3.18	3.21	3.18	2.88
SCR[%]	10.14	10.40	10.77	10.78	9.85	9.85	9.89	9.93	9.95	10.33	10.03	10.05	10.11	10.15
SPF _{SHPP+pen} [-]	2.79	2.78	2.79	2.79	2.47	2.44	2.42	2.73	2.76	2.79	2.51	2.53	2.45	2.02
f _{sav,CO₂} [%]	49.21	48.99	49.17	49.18	42.68	42.00	41.54	48.06	48.66	49.22	43.87	44.1	42.33	30.56
RIB[%]	45.34	45.75	45.37	45.36	28.92	28.73	29.36	44.26	37.28	46.44	30.17	29.43	29.74	37.40
GSC _{abs} [-]	1.02	1.02	1.02	1.02	0.95	0.95	0.95	1.02	0.99	1.03	0.95	0.96	0.96	0.92
t _{T<} [h]	120	162.01	119.75	119.74	163.69	112.36	110.04	95.26	148.80	127.67	279.88	193.57	169.58	410.66
n _{starts} [-]	1633	1660	1638	1639	742	794	793	1165	1108	1156	917	984	940	747
Scaled Total [-]	0.506	0.516	0.628	0.630	0.634	0.638	0.632	0.529	0.616	0.595	0.603	0.639	0.631	0.354
Ranking [-]	13	12	7	6	3	2	4	11	8	10	9	1	5	14



Table 9
Classification of evaluation values.

Evaluation Indicator	Value Range	System Operator supportive if...	Grid Operator supportive if...
SSR	0 – 100%	high value	-
SCR	0 – 100%	high value	-
SPF _{SHPP+pen}	> 0	high value	-
f _{sav,CO₂} ^a	0 – 100%	high value	-
RIB	0 – 100%	low value	low value
GSC _{abs}	> 0	-	low value
t _{T<}	≥ 0min	low value	-
n _{starts}	≥ 0	low value	low value

^a Only applies if $E_{el,WP} < \frac{E_{ref}GW_{P_{ref}}}{GW_{P_{el}}}$.

individual evaluations were carried out for single-family houses with different degrees of renovation and HP systems with and without PV battery storage systems and, on the other hand, for a RRA. The results show that among the equally weighted valuation variables considered, the strategies based on control and day-ahead electricity prices simultaneously have the potential for the best and worst compromise for grid operators and system operators. The choice of switching limits in the course of the price signal is crucial. Accordingly, local conditions should be taken into account when designing the price signals.

The comparison of the heat map of PRBC1 and PRBC4 shows that an even distribution of OS 2 and OS 3 in the middle value range produces a better result (rank 1) than the predominant operation in the boosted state OS 3 (rank 14) (see Fig. 17 and Fig. 19).

With the amended Section 14a of the EnWG, that came into force on January 1, 2024, it obliges DGO and end consumers with controllable consumption devices to participate to avoid grid congestion.

The operating strategies presented here are based either on rule-based controls or time-based profiles and can therefore be implemented easily and quickly in the field compared to optimization-based operating strategies, which also have higher hardware requirements.

The fulfillment value of the best operating strategy (PRBC2) with the key figures considered here for the representative residential area is 63.9%, while the value for the reference operating strategy (Ref.), in which the heat pump is operated exclusively in SG-Ready Mode 2, is only 50.6%. The worst operating strategy PRBC4 only achieves a degree of fulfillment of 35.4%.

In addition, the consumer receives benefits. Future studies will take a closer look at the effects of these benefits for system operators and the DGO.

In recent years, integrated inverter technology has become established in modulating heat pumps. The main difference between conventional and modulating HPs is the power consumption. Ordinary HPs

draw electricity when the compressor is active. This is switched on and off at regular intervals. This results in regular consumption peaks which, depending on the simultaneity, can put a strain on the grid. Modulating heat pumps, on the other hand, can modulate the output. This means that the required output, i.e. the power consumption, can be regulated continuously. The output is constantly adapted to the current heating requirement. The positive effects of the even power consumption adapted to the heating requirement will also be examined in more detail in future work.

Another technological advance in HPs is the room cooling function. This is done passively with brine/water HPs or actively with air/water HPs by switching on the refrigerant compressor. Due to the improved temporal overlap of PV generation output and cooling demand, positive effects for the system operator are to be expected here. Whether there are also effects for the grid operator remains to be clarified in future research.

By participating in the energy markets with the help of aggregators, additional income can also be generated for the homeowner by providing grid-stabilizing ancillary services [68,69], which have not yet been taken into account here.

CRedit authorship contribution statement

J. Meiers: Writing – original draft, Visualization, Conceptualization. **M. Ortleb:** Methodology. **D. Jonas:** Methodology. **L. Tadayon:** Methodology. **G. Frey:** Writing – original draft, Supervision, Conceptualization.

Declaration of competing interest

The authors declare that they have no known competing financial interests or personal relationships that could have appeared to influence the work reported in this paper.

Data availability

Data will be made available on request.

References

- [1] V. Duscha, A. Denishchenkova, J. Wachsmuth, Achievability of the Paris agreement targets in the EU: demand-side reduction potentials in a carbon budget perspective, Climate Policy 19 (2019) 161–174.
- [2] N. Damianakis, G.R.C. Mouli, P. Bauer, Y. Yu, Assessing the grid impact of electric vehicles, heat pumps & PV generation in Dutch LV distribution grids, Appl. Energy 352 (2023) 121878.
- [3] Global installed energy storage capacity by scenario, 2023 and 2030, 2024. Licence: CC BY 4.0, Last updated 25 April 2024.

- [4] European Parliament, Directive (EU) 2018/2001 of the European Parliament and of the Council of 11 December 2018 on the promotion of the use of energy from renewable sources, *Off. J. Eur. Union L* 328 (2018) 82–209.
- [5] Bundesregierung Deutsche, Bundesministerium für Wirtschaft und Klimaschutz, in: Klimaschutzbericht 2022, Berlin, 2022.
- [6] M. Ortleb, J. Meiers, D. Jonas, G. Frey, Operation strategies using the smart grid ready interface in solar heat pump systems, in: 2022 IEEE 1st Industrial Electronics Society Annual On-Line Conference (ONCON), pp. 1–6.
- [7] J. Meiers, G. Frey, Ready4SmartHeat-Wirkung der Wärmepumpensteuerung mit Smart-Grid-Ready-Schnittstelle für ein repräsentatives Wohngebiet, in: *Automation 2024: AI Beats Automation? (25. Leitkongress der Mess und Automatisierungstechnik)*, in: VDI Wissensforum GmbH, vol. VDI-Berichte 2437, VDI Verlag, Düsseldorf, 2024, pp. 869–881.
- [8] M. Shabanzadeh, M.P. Moghaddam, What is the smart grid? Definitions, perspectives, and ultimate goals, in: 28th International Power System Conference (PSC), Tehran, Iran, pp. 1–10.
- [9] Bundesnetzagentur für Elektrizität, Gas, Telekommunikation, Post und Eisenbahnen (BNetzA), Bundeskartellamt (BKartA), Monitoringbericht 2022, 2022.
- [10] European Union Agency for the Cooperation of Energy Regulator (ACER), Council of European Energy Regulators (CEER), Annual report on the results of monitoring the internal electricity and natural gas markets in 2021-energy retail and consumer protection volume, 2022.
- [11] D. Kolokotsa, The role of smart grids in the building sector, *Energy Build.* 116 (2016) 703–708.
- [12] European Union, Directive (EU) 2018/844 of the European Parliament and of the Council of 30 May 2018 amending Directive 2010/31/EU on the energy performance of buildings and Directive 2012/27/EU on energy efficiency, 2018.
- [13] I.A. Campodonico Avendano, K. Heimar Andersen, S. Erba, A. Moazami, M. Aghaei, B. Najafi, A novel framework for assessing the smartness and the smart readiness level in highly electrified non-residential buildings: a Norwegian case study, *Energy Build.* 314 (2024) 114234.
- [14] B. Ramezani, M.G. da Silva, N. Simões, Application of smart readiness indicator for Mediterranean buildings in retrofitting actions, *Energy Build.* 249 (2021) 111173.
- [15] K. Wissler, Gebäudeautomation in Wohngebäuden (Smart Home): Eine Analyse der Akzeptanz, Vieweg, Wiesbaden, 2018.
- [16] Building Automation and Control Systems (BACS), Deutsche Norm, vol. DIN EN ISO 16484, Beuth, Berlin, 2004.
- [17] Bundesnetzagentur, Smart Grid and Smart Market: Eckpunktepapier der Bundesnetzagentur zu den Aspekten des sich verändernden Energieversorgungssystems, Bonn, 2011.
- [18] Smart grids in Germany: Fields of action for distribution system operators on the way to smart grids, in: BDEW - Bundesverband der Energie- und Wasserwirtschaft e. V. und ZVEI - Zentralverband Elektrotechnik- und Elektronikindustrie e.v., Berlin and Frankfurt am Main, Germany, 2012.
- [19] Bundesverband Wärmepumpe, Regularium für das Label “SG Ready” für elektrische Heizungs- und Warmwasserärmepumpen, 2020.
- [20] D. Fischer, Integrating Heat Pumps into Smart Grids, Ph.D. thesis, KTH, Energy Technology, 2017.
- [21] D. Fischer, M.-A. Triebel, O. Selinger-Lutz, A concept for controlling heat pump pools using the smart grid ready interface, in: 2018 IEEE PES Innovative Smart Grid Technologies Conference Europe (ISGT-Europe), IEEE, pp. 1–6.
- [22] D. Fischer, T. Wolf, M.-A. Triebel, Flexibility of heat pump pools: The use of sg-ready from an aggregator's perspective, in: 12th IEA Heat Pump Conference, pp. 1–12.
- [23] F. Lilliu, T.B. Pedersen, L. Siksnys, Heat flexoffers: a device-independent and scalable representation of electricity-heat flexibility, in: Proceedings of the 14th ACM International Conference on Future Energy Systems, pp. 374–385.
- [24] T. Kemmler, R. Maier, C. Widmann, B. Thomas, Using a thermal energy storage to provide flexibility for heat pump optimization control with rapid control prototyping and sg ready standard, in: Proceedings of the 13th International Renewable Energy Storage Conference 2019 (IRES 2019).-(Atlantis Highlights in Engineering; 4), Atlantis Press, pp. 132–136.
- [25] S. Göbel, C. Vering, D. Müller, Experimental investigation of rule-based control strategies for hybrid heat pump systems using the smart grid ready interface', in: Proceedings of ECOS 2022, 2022.
- [26] S. Baraskar, D. Günther, J. Wapler, M. Lämmle, Analysis of the performance and operation of a photovoltaic-battery heat pump system based on field measurement data, *Sol. Energy Adv.* 4 (2024) 100047.
- [27] J.-C. Hadorn, Solar and Heat Pump Systems for Residential Buildings, John Wiley & Sons, 2015.
- [28] D. Jonas, Model-based analysis of solar and heat pump systems for the energy supply of residential buildings, Ph.D. thesis, Saarland University, Germany, 2023.
- [29] E. Frank, M. Haller, S. Herkel, J. Ruschenburg, Systematic classification of combined solar thermal and heat pump systems, in: Proceedings of the EuroSun 2010 Conference, Graz, Austria.
- [30] D. Jonas, Visualization of energy flows in pvt systems. A visualization scheme for the uniform representation of combined electrical and thermal energy flows in pvt systems, Report D4, IEA SHC Task 60 PVT Systems, International Energy Agency, Solar Heating and Cooling Programme, 2019.
- [31] S. Poppi, N. Sommerfeldt, C. Bales, H. Madani, P. Lundqvist, Techno-economic review of solar heat pump systems for residential heating applications, *Renew. Sustain. Energy Rev.* 81 (2018) 22–32.
- [32] L.G. Swan, V.I. Ugursal, Modeling of end-use energy consumption in the residential sector: a review of modeling techniques, *Renew. Sustain. Energy Rev.* 13 (2009) 1819–1835.
- [33] M. Kavgić, A. Mavrogianni, D. Mumović, A. Summerfield, Z. Stevanović, M. Djurović-Petrović, A review of bottom-up building stock models for energy consumption in the residential sector, *Build. Environ.* 45 (2010) 1683–1697.
- [34] V.-G. Energietechnik, Reference load profiles of single-family and multi-family houses for the use of chp systems, 2008.
- [35] Bundesverband Wärmepumpe, Branchenstudie 2023: Marktentwicklung - Prognose - Handlungsempfehlungen, 2023.
- [36] Statistisches Bundesamt (Destatis), Wohnungen nach Baujahr, 2020.
- [37] H. Cischinsky, N. Diefenbach, Datenerhebung wohngebäudebestand 2016, 2018.
- [38] D. Energie-Agentur, Dena-Gebäudereport kompakt...: Statistiken und Analysen zur Energieeffizienz im Gebäudebestand, Deutsche Energie-Agentur (dena), 2019.
- [39] R. Dott, M.Y. Haller, J. Ruschenburg, F. Ochs, J. Bony, The reference framework for system simulations of the IEA SHC Task 44/HPP Annex 38 Part B: buildings and space heat load, International Energy Agency, 2013.
- [40] EuPD Research Sustainable Management GmbH, 89 Prozent des solarpotenzials auf deutschen ein- und zweifamilienhäusern sind noch ungenutzt, 2021.
- [41] E3DC, die sg ready-funktion der s10 hauskraftwerke, 2017.
- [42] T. Tjaden, J. Weniger, V. Quaschnig, Richtige dimensionierung von photovoltaik, wärmepumpen und pufferspeichern, C.A.R.M.E.N.-Symposium, 2017.
- [43] C. Fünfgeld, R. Tiedemann, Anwendung der repräsentativen VDEW-Lastprofile: step-by-step, VDEW, 2000.
- [44] D. Fischer, J. Bernhardt, H. Madani, C. Wittwer, Comparison of control approaches for variable speed air source heat pumps considering time variable electricity prices and pv, *Appl. Energy* 204 (2017) 93–105.
- [45] Bundesnetzagentur für Elektrizität, Gas, Telekommunikation, Post und Eisenbahnen (BNetzA), Smart - strommarktdaten: Großhandelspreise, 2023.
- [46] Entsoe, Transparency platform, 2023.
- [47] K. Rheinberger, Dsm-data, 2023.
- [48] D. Jonas, D. Theis, G. Frey, Implementation and experimental validation of a photovoltaic-thermal (pvt) collector model in trnsys, in: Proceedings of the 12th International Conference on Solar Energy for Buildings and Industry (EuroSun2018), vol. 10, Rapperswil, Switzerland, pp. 798–809.
- [49] M. Haller, R. Dott, J. Ruschenburg, F. Ochs, J. Bony, Iea-shc task 44 subtask c technical report, in: The Reference Framework for System Simulations of the IEA SHC Task 44/HPP Annex 38: Part A: General Simulation Boundary Conditions, 2012.
- [50] U.I. Dar, I. Sartori, L. Georges, V. Novakovic, Advanced control of heat pumps for improved flexibility of net-zeb towards the grid, *Energy Build.* 69 (2014) 74–84.
- [51] P. Götz, J. Henkel, T. Lenck, Zusammenhang von strombörsenpreisen und endkundenpreisen, Studie im Auftrag der Agora Energiewende, vol. 7, 2013, p. 2016.
- [52] K. Klein, R. Langner, D. Kalz, S. Herkel, H.-M. Henning, Grid support coefficients for electricity-based heating and cooling and field data analysis of present-day installations in Germany, *Appl. Energy* 162 (2016) 853–867.
- [53] M.Y. Haller, R. Dott, J. Ruschenburg, F. Ochs, J. Bony, The reference framework for system simulations of the IEA SHC Task 44/hpp annex 38 part a: General simulation boundary conditions, A technical report of subtask CReport C1 Part A, International Energy Agency, 2013.
- [54] Deutsches Institut für Normung, Din 1946, raumluftechnik - gesundheitstechnische anforderungen, 2019.
- [55] M. Akmal, B. Fox, J.D. Morrow, T. Littler, Impact of heat pump load on distribution networks, *IET Gener. Transm. Distrib.* 8 (2014) 2065–2073.
- [56] P. Perrin, Simulationsbasierte Analyse der Einflussfaktoren auf Betriebszahlen von Wärmepumpenanlagen, Ph.D. thesis, Dissertation, Technische Universität Braunschweig, Braunschweig, 2012.
- [57] E. Rossi di Schio, V. Ballerini, The scope of an air source heat pump: comparison between on-off and inverter heat pump, *JP J. Heat Mass Transf.* 24 (2021) 79–86.
- [58] K.-J. Chae, X. Ren, Flexible and stable heat energy recovery from municipal wastewater treatment plants using a fixed-inverter hybrid heat pump system, *Appl. Energy* 179 (2016) 565–574.
- [59] Solar Energy Laboratory, University of Wisconsin, TRNSYS - a Transient System Simulation Program, 2014.
- [60] D. Jonas SHP-SimLib, A library of solar and heat pump subsystem simulation models in TRNSYS, 2023.
- [61] M. Wetter, T.S. Nouidui, P. Haves, Building Controls Virtual Test Bed (BCVTB), 2016, version 1.6.0.
- [62] The Math Works Inc., Matlab, 2020.
- [63] D. Jonas, Type 835, PVT-Modell für TRNSYS, 2019.
- [64] M. Wetter, T. Afjei, Trnsys Type 401 Compressor Heat Pump Including Frost and Cycle Losses, Zentralschweizerisches Technikum, Luzern, Horw, Switzerland, 1997.
- [65] H. Drück, Type 340, MULTIPORT Store-Modell für TRNSYS, 2006.
- [66] Viessmann, Installation and service instructions for contractors, vitocal 200-g, typ bwc 201.b06 to b17, type bwc-m 201.b06 to b10, 2020.
- [67] Enphase Energy Inc, Installations- und Konfigurationshandbuch, SG Ready – Installation und Konfiguration, Viessmann Vitocal 200-S Wärmepumpensystem, 2023.
- [68] X. Nie, S.A. Mansouri, A. Rezaee Jordehi, M. Tostado-Véliz, A two-stage optimal mechanism for managing energy and ancillary services markets in renewable-based transmission and distribution networks by participating electric vehicle and demand response aggregators, *Int. J. Electr. Power Energy Syst.* 158 (2024) 109917.

- [69] M. Zhang, Q. Wu, T.B.H. Rasmussen, X. Yang, J. Wen, Heat pumps in Denmark: current situation in providing frequency control ancillary services, *CSEE J. Power Energy Syst.* 8 (2022) 769–779.



Josef Meiers graduated with a Diplom Ingenieur degree (M.Sc.) in Mechatronics from Saarland University, Saarbrücken, Germany, in 2013. From 2013 he is a research assistant at the Chair of Automation and Energy Systems, Saarland University, where he is currently pursuing the Ph.D. degree. His active research interests include Advanced Control of renewable energy systems with battery storage and solar heat pump systems using Digital Twin.



Mitja Ortleb has been working as a research assistant at the Chair of Automation and Energy Systems at Saarland University since completing his B.Sc. degree in Systems Engineering at Saarland University, Saarbrücken, Germany in 2022. In 2025 he will complete his M.Sc. in the same course of study. His research focuses on the investigation of control strategies and the development of different system combinations for heat pumps and renewable energy systems.



Danny Jonas graduated with Ph.D. degree from Saarland University, Saarbrücken, Germany, in 2024. From 2015 to 2019, he was a research assistant at the Chair of Automation and Energy Systems, Saarland University, where his active research interests focused on the model-based analysis of solar and heat pump systems for the energy supply of residential building. He is currently freelance engineer and scientist.



Leon Tadayon received his M.S. degree in systems engineering at the Saarland University, Saarbrücken, Germany in 2024. He is currently working toward the Ph.D. degree in systems engineering and is a research assistant at the Chair of Automation and Energy Systems, Saarland University. His research interest includes optimal operation of battery energy storage systems.



Georg Frey received the Diplom Ingenieur (M.Sc.) degree in electrical engineering/control engineering from the Karlsruhe Institute of Technology, Karlsruhe, Germany, in 1996 and the Doktor-Ingenieur (Ph.D.) from the University of Kaiserslautern-Landau, Kaiserslautern, Germany, in 2002. He was an Associate Professor with the University of Kaiserslautern-Landau and was also with the German Research Center for Artificial Intelligence. Since 2009, he is a Full Professor and holds the Chair of Automation and Energy Systems at Saarland University. His research interests include modeling, simulation, and optimization of complex automation and energy systems, industrial security, and reconfigurable systems.